



# Effect of Nickel-Aluminum Trioxide/Titanium Dioxide Nanocomposites on Photo-oxidation of Olive Mill Wastewater

**Oztekin R\***

Department of Environmental Engineering, Dokuz Eylul University, Turkey

**\*Corresponding author:** Post-Dr. Rukiye Oztekin, (Ph.D.) Department of Environmental Engineering, Dokuz Eylul University, Tinaztepe Campus, 35160 Buca/Izmir, Turkey, Tel: +902323017119; Email: rukiyeoztekin@gmail.com

**Research Article**

**Volume 7 Issue 2**

**Received Date:** June 07, 2024

**Published Date:** July 10, 2024

**DOI:** 10.23880/aabsc-16000226

## Abstract

In this study, the magnetic nickel (Ni) doped aluminium trioxide (aluminium oxide or alumina,  $\text{Al}_2\text{O}_3$ ) based titanium dioxide ( $\text{TiO}_2$ ) [ $\text{Ni-Al}_2\text{O}_3/\text{TiO}_2$ ] nanocomposites (NCs) was used for the photocatalytic oxidation (photo-oxidation) of pollutant parameters {chemical oxygen demand (COD) components [ $\text{COD}_{\text{total}}$ ,  $\text{COD}_{\text{dis}}$ ,  $\text{COD}_{\text{inert}}$ ]}, toxic polyphenols [catechol, 3-hydroxybenzoic acid, tyrosol, 4-hydroxybenzoic acid, 4-hydroxyphenylacetic acid, 3-hydroxyphenylpropionic acid, 4-hydroxyphenylpropionic acid, 3,4-dihydroxyphenylethanol, 3,4-dihydroxyphenylacetic acid], and toxic polyaromatics [aniline, 4-nitroaniline, o-toluidine, o-anisidine, benzene, nitrobenzene, ethylbenzene, 3,6-bis(dimethylamino)durene, benzidine, dimethylaniline, 3,3-dichlorobenzidine]} from the olive mill effluent wastewaters (OMW), at different mass ratios of  $\text{Al}_2\text{O}_3$ ,  $\text{TiO}_2$  and Ni (1%/5%/10%; 10%/1%/5% and 1%/10%/5%), at increasing photooxidation times (10, 30, 60, 100 and 120 min), at different Ni/ $\text{Al}_2\text{O}_3/\text{TiO}_2$  photocatalyst concentrations (50, 250, 500 and 1000 mg/l), pH values (4.0-7.0-9.0 and 10.0) and temperatures (15°C, 25°C, 50°C and 80°C), under 500 W ultraviolet visible (UV-vis) and 50 W sun lights irradiations, respectively. The acute toxicity assays were operated with Microtox (*Aliivibrio fischeri* also called *Vibrio fischeri*) and *Daphnia magna* acute toxicity tests. The significance of the correlations between data of all experimental samples were determined using the Analysis of Variance (ANOVA) test statistics. Under the optimized conditions, the maximum  $\text{COD}_{\text{dis}}$ , total phenol and total aromatic amines (TAAs) photooxidation yields were 98%, 88%, 94%, respectively, at pH=9.0, at 500 mg/l Ni/ $\text{Al}_2\text{O}_3/\text{TiO}_2$  NCs, under 500 W UV-vis light, after 100 min photooxidation time, at 50°C, respectively. The photooxidation yields in OMW under sun light was lower than the photooxidation yields in the OMW under UV-vis light. 94.44% maximum Microtox acute toxicity yield was found in Ni/ $\text{Al}_2\text{O}_3/\text{TiO}_2$  NCs=500 mg/l after 150 min photooxidation time, at 60°C. 90% maximum *Daphnia magna* acute toxicity removal was obtained in Ni/ $\text{Al}_2\text{O}_3/\text{TiO}_2$  NCs=500 mg/l after 150 min photooxidation time, at 60°C. Microtox acute toxicity test was more sensitive than *Daphnia magna* acute toxicity assay.

**Keywords:** Acute Toxicity Assays (*Aliivibrio Fischeri*, *Daphnia Magna*); Magnetic Nickel Coated Aluminium Trioxide Based Titanium Dioxide Nanocomposites; Olive Mill Effluent Wastewater; Photocatalytic Oxidation (Photo-oxidation); Polyaromatics and Polyphenols; Ultraviolet Visible and Sun Light Irradiations

## Abbreviations

Al<sub>2</sub>O<sub>3</sub>: Aluminium Trioxide (Aluminium Oxide or Alumina); TiO<sub>2</sub>: Titanium Dioxide; Ni: Nickel; Ni/Al<sub>2</sub>O<sub>3</sub>/TiO<sub>2</sub> NCS: Nickel Doped Aluminium Trioxide Based Titanium Dioxide Nanocomposites; OMW: Olive Mill Effluent Wastewaters; UV-vis: Ultraviolet Visible Irradiation; ANOVA: Analysis of Variance; TAAs: Total Aromatic Amines; NCS: Nanocomposites; COD: Chemical Oxygen Demand; COD Components: COD<sub>total</sub>, COD<sub>dissolved</sub>, COD<sub>inert</sub>; <sup>13</sup>CNMR: Carbon-13 (C<sub>13</sub>) Nuclear Magnetic Resonance Spectroscopy; C: Carbon; N<sub>2</sub>(g): Nitrogen Gas; O<sub>2</sub>(g): Oxygen Gas; US: Ultrasound; OH●: Hydroxyl Radicals; NPs: Nanoparticles; DO: Dissolved Oxygen; Ni(NO<sub>3</sub>)<sub>2</sub> · 6H<sub>2</sub>O: Nickel Nitrate Hexahydrate; He(g): Helium Gas; GC: Gas Chromatography; ORP: Oxidation Reduction Potential; BOD<sub>5</sub>: Biochemical Oxygen Demand-5 Days; COD<sub>total</sub>: Chemical Oxygen Demand-Total; COD<sub>dissolved</sub>: Chemical Oxygen Demand-Dissolved; TSS: Total Suspended Solids; Total-N: Total-Nitrogen; NH<sub>3</sub>-N: Ammonia-Nitrogen; NO<sub>3</sub>-N: Nitrate-Nitrogen; NO<sub>2</sub>-N: Nitrite-Nitrogen; Total-P: Total-Phosphorus; PO<sub>4</sub>-P: Phosphate-Phosphorus; COD<sub>inert</sub>: Chemical Oxygen Demand-Inert; HPLC: High-Pressure (or Performance) Liquid Chromatography; H<sub>2</sub>O: Water; DL: Detection Limit; QL: Quantification Limit; SD: Standard Deviation; CO<sub>2</sub>●: Carboxyl Radicals; OH<sub>2</sub>●: Hydroperoxyl Radicals; PECS: Pulsed Electric Current Sintering; PLS: Pressureless Sintering; 25°C: Room Temperature; CO<sub>3</sub><sup>2-</sup>: Carbonate Ions; CO<sub>3</sub>●: Carbonate Radical; O<sub>2</sub>●<sup>-</sup>: Superoxide Radical; e<sup>-</sup>: electrons; VB: Valence Band; CB: Conduction Band; H<sub>2</sub>O<sub>2</sub>: Hydrogen Peroxide; O<sub>2</sub>●: Oxygen Radicals; Ce-TZP/Al<sub>2</sub>O<sub>3</sub>: Cerium-Tetragonal Zirconia Polycrystal (TZP) Based Aluminium Trioxide; XRD: X-Ray Diffractometry; TEM: Transmission Electron Microscopy; COOH: Carboxyl Groups; CHO: Carbohydrates Groups; H-bonds: Hydrogen Bonds.

## Introduction

Water, the source of life, is considered the most fundamental element for the survival of humans, animals and plants. Olive oil production is also responsible for various environmental pollutants such as soil pollution, underground seepage, water body pollution and odor emissions, etc., which occur due to poor waste management practices [1]. Agro-industrial wastewaters such as OMW are among the strongest industrial effluents and increasing concern has been expressed about their treatment and safe disposal, since they cause considerable environmental problems (coloring of natural waters, a serious threat to aquatic life, pollution in surface and ground waters, alterations in soil quality, phytotoxicity and odor nuisance) particularly in the Mediterranean Sea region due to its high organic COD, polyphenol, aromatic amines concentration and organic content [2-4]. Recently, phenols, fatty acids

and volatile acids have been potentially serious dangers to environmental health; They have distinct antimicrobial and phytotoxic properties and show high toxicity values due to their long alkyl chains [5,6].

OMW dilution; It is generally used before biological treatments to reduce the toxicity of OMW wastewater, which contains complex toxic and refractory pollutants against microorganisms. In contrast, evaporation and sedimentation result in a concentrated OMWW (approximately 70–75% more concentrated) thanks to both phase separation/dehydration and organic matter degradation [7,8]. Additionally, solar distillation applied to OMW can remove 80% COD from the distillate in 9 days and maintain 25% H<sub>2</sub>O content [9]. Other strategies, mainly consisting of irreversible heat treatments, have also been investigated in the literature from different perspectives. This is the case with the “zero waste approach”, which requires reducing the amount of waste to a minimum level, and with combustion and pyrolysis, which provide “energy recovery”. This is the case with combustion and pyrolysis that require a reduced volume of waste and provide energy recovery. However, unfortunately, in the vast majority of these approaches; Expensive facilities are needed, toxic substances are released into the atmosphere, and therefore an OMW pre-concentration stage is needed [10,11].

In recent years, in studies in the literature; Advanced oxidation processes (AOPs), including photolysis, photo-oxidation, Fenton, and photo-Fenton reaction, have emerged as promising alternatives for simplicity and high organic removal efficiencies [12-18]. OMW adsorption on activated clay results in an additional 71% COD reduction. However, it requires special focus on the adsorption/desorption balance, as organic and phenolic properties begin to desorb after a certain contact time. For OMW pollutions removals, combination of process stages; namely, sedimentation, centrifugation, filtration, and adsorption on activated carbon have been reported to result in a maximum 94% phenol reduction and 83% organic matter removal [19]. Justino CI, et al. [20] studied the combination of fungi *Pleurotus sajor caju* and photo-Fenton oxidation process. Accordingly, treatment with *Pleurotus sajor caju* fungi confirmed reduced OMW toxicity towards *Daphnia longispina*, and resulting in an overall yield of 72.9% total phenolic compound removal and 77% COD reduction [20].

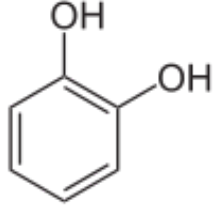
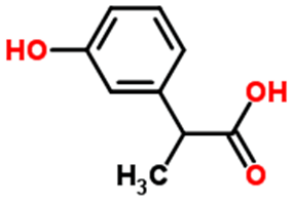
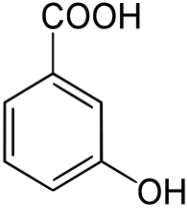
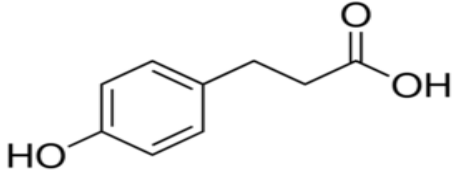
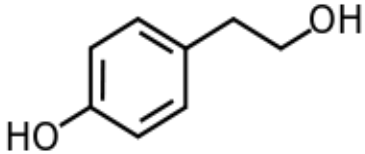
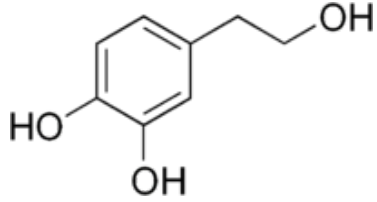
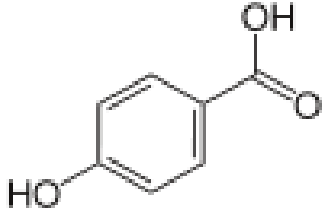
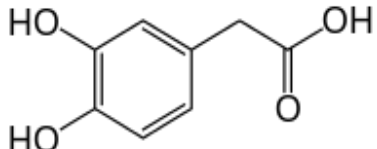
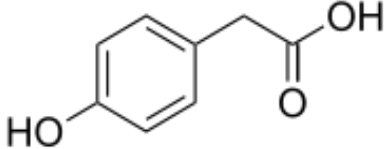
The concentration of phenolic compounds in the OMW may vary from as low as 0.05-0.2 g/l to as high as 10 g/l depending on the type and origin of the effluent [6,21]. The TAAs in the OMW are known to be carcinogenic and toxic. Some aromatic amines containing the azo bonds (–N=N–) have complex structure and are resistant to biodegradation under aerobic conditions [22,23]. The Carbon-13 (C13)

nuclear magnetic resonance spectroscopy (CNMR) of spectra of the OMW showed that aliphatic carbon substituted by oxygen and nitrogen and including the methoxyl groups of aromatic ethers (50 and 110 mg/l), double bonded or aromatic carbon (110 and 160 mg/l) and carboxylic carbon in ester or amide (160-200 mg/l). The resonances observed between 40 and 105 mg/l were generated by carbons bound directly to an oxygen heteroatom as in alcohols and carbohydrates or nitrogen as in amines, amino acids and amides (C-N, N-H) [22]. The aromatic region (110–160 mg/l) can be divided into three parts, one between 110 and 130 mg/l for unsubstituted aromatic carbons, another between 130 and 145 mg/l for C-substituted aromatic carbons and the last between 145 and 160 mg/l for N substituted aromatic organics [23,24].

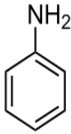
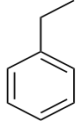
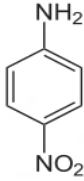
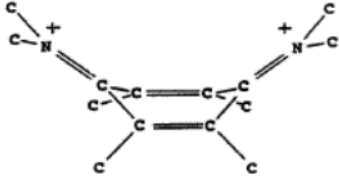
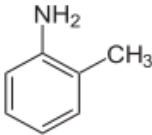
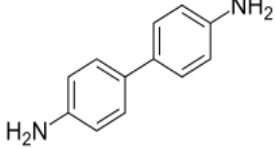
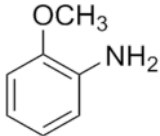
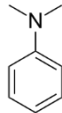

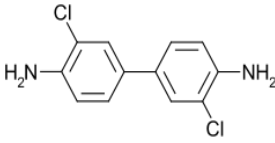
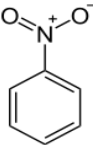
Significant numbers of studies were focused on the efficient treatment of the OMW including various chemical, physical, physicochemical and biological treatments or combinations of them [4,5,21,25-27]. Over the past few years, various advanced oxidative processes, and many hybrid technologies, were used to completely or partially degrade the COD and the polyphenols [28]. Usually, the OMW is inappropriate for direct biological treatment and the alternative treatment technologies mentioned above did not give sufficient removals for pollution parameters (COD<sub>dis</sub>, phenol, color and aromatic amines). Even though, all of these methods are practicable and effective, they cannot be used ubiquitously with high efficiency and may generate hazardous by-products [28]. Recently, significant interest has been shown in the application of ultrasound (US) for the degradation of the OMW [2,29]. Hydrophobic compounds with high volatility are easily and directly destroyed inside the cavitation bubbles [30]. Hydrophilic organic compounds are indirectly decomposed mainly through the reaction with hydroxyl radicals (OHL) that is produced during cavitation process. The highly reactive OHL could diffuse from the cavitation bubbles to the interfacial region and bulk solution when large temperature gradient exist [30]. There are three potential reaction zones in sonochemistry; i.e. inside of the cavitation bubble, interfacial liquid region between cavitation bubbles and bulk liquid, and in the bulk solution [30]. The collapse of cavitation bubbles near the micro-particle surface will generate high-speed microjets of liquid in the order of 100 m/s [30]. This will subsequently produce ultrasonic asymmetric shock wave upon implosion of

cavitation bubbles which may cause direct erosion (damage) on the particle's surface and de-aggregation of particles to hinder agglomeration. Consequently, it will experience a decrease in particle size and an increase in reactive surface area available for the subsequent reaction. The nanoparticles (NPs) with the size less than that of cavitation bubbles have higher cavitation erosion resistant and are easier to approach the interfacial region (bubbles surface) during the expansion cycles of US [30]. It was observed synergetic effects with the addition of various metal oxides with US to enhance the rate of degradation efficiency of organic pollutants via increasing the OHL. This increasing the rate of degradation of the organic compounds in wastewaters. The sonication of organic pollutants in the presence of some metal oxides (this reaction could be named as heterogeneous sonication) can easily occur in the interfacial region where very high concentration of OHL is achieved after the bubbles collapse [30]. US will induce the splitting of water molecules with the presence of dissolved oxygen (DO) [30]. In these reactions, ')))' denotes the ultrasonic irradiation.

In this present study, Ni/Al<sub>2</sub>O<sub>3</sub>/TiO<sub>2</sub> NCs was used for the photooxidation of pollutant parameters {COD components [COD<sub>total</sub>, COD<sub>dissolved</sub>, COD<sub>inert</sub>], polyphenols [catechol, 3-hydroxybenzoic acid, tyrosol, 4-hydroxybenzoic acid, 4-hydroxyphenylacetic acid, 3-hydroxyphenylpropionic acid, 4-hydroxyphenylpropionic acid, 3,4-dihydroxyphenylethanol, 3,4-dihydroxyphenylacetic acid (Table 1), and polyaromatics [aniline, 4-nitroaniline, o-toluidine, o-anisidine, benzene, nitrobenzene, ethylbenzene, 3,6-bis(dimethylamino)durene, benzidine, dimethylaniline, 3,3-dichlorobenzidine] Table 2 from the OMW at different operational conditions such as at different mass ratios of Al<sub>2</sub>O<sub>3</sub>, TiO<sub>2</sub> and Ni (1%/5%/10%; 10%/1%/5% and 1%/10%/5%), at increasing photooxidation times (10, 30, 60, 100 and 120 min), at different Ni/Al<sub>2</sub>O<sub>3</sub>/TiO<sub>2</sub> photocatalyst concentrations (50, 250, 500 and 1000 mg/l), pH values (4.0-7.0-9.0-10.0) and temperatures (15°C, 25°C, 50°C and 80°C), under 500 W UV-vis and 50 W sun lights irradiations, respectively. The acute toxicity assays were operated with Microtox (*Aliivibrio fischeri* also called *Vibrio fischeri*) and *Daphnia magna* acute toxicity tests. Furthermore, the toxicity of the OMW to *Daphnia magna* (water flea) and to *Aliivibrio fischeri* (bacteria) were correlated. The significance of the correlations between data of all experimental samples were calculated using the ANOVA statistical analysis.

No	The Chemical Formulas of Polyphenols		
	Polyphenols names	No	Polyphenols names
1	 <p>catechol</p>	6	 <p>3-hydroxyphenylpropionic acid</p>
2	 <p>3-hydroxybenzoic acid</p>	7	 <p>4-hydroxyphenylpropionic acid</p>
3	 <p>tyrosol</p>	8	 <p>3,4-dihydroxyphenylethanol</p>
4	 <p>4-hydroxybenzoic acid,</p>	9	 <p>3,4-dihydroxyphenylacetic acid.</p>
5	 <p>4-hydroxyphenylacetic acid</p>		

**Table 1:** The chemical formulas of polyphenols (catechol, 3-hydroxybenzoic acid, tyrosol, 4-hydroxybenzoic acid, 4-hydroxyphenylacetic acid, 3-hydroxyphenylpropionic acid, 4-hydroxyphenylpropionic acid, 3,4-dihydroxyphenylethanol, 3,4-dihydroxyphenylacetic acid) in the OMW with photo-oxidation process under UV-vis and sun lights irradiations.

No	The Chemical Formulas of Polyaromatics		
	Polyaromatics names	No	Polyaromatics names
1	 aniline	7	 ethylbenzene
2	 4-nitroaniline	8	 3,6-bis(dimethylamino)durene
3	 o-toluidine	9	 benzidine
4	 o-anisidine	10	 dimethylaniline
5	 benzene	11	 3,3-dichlorobenzidine
6	 nitrobenzene		

**Table 2:** The chemical formulas of polyaromatics [aniline, 4-nitroaniline, o-toluidine, anisidine, benzene, nitrobenzene, ethylbenzene, 3,6-bis(dimethylamino)durene, benzidine, dimethylaniline, 3,3-dichlorobenzidine] in the OMW with photooxidation process under UV-vis and sun lights irradiations.

## Materials and Methods

### Raw Wastewater

The characterization of raw OMW taken from the influent of a olive oil production industry in Izmir, Turkey is given in Table 3. This plant is operated with a three phase olive oil extraction process.

Parameters	Values		
	Minimum	Medium	Maximum
pH <sub>0</sub>	3.9 ± 0.14	4.4 ± 0.16	4.9 ± 0.17
DO <sub>0</sub> ( mg/l)	0.01 ± 0.0004	0.06 ± 0.0021	0.11 ± 0.004
ORP (mV)	121 ± 4.24	128 ± 4.48	135 ± 4.73
TSS (mg/l)	56.3 ± 1.97	59.6 ± 2.1	62.8 ± 2.2
COD <sub>total</sub> (mg/l)	98760 ± 3456.6	112085 ± 3923	125410 ± 4389.4
COD <sub>dis</sub> (mg/l)	86267 ± 3019.4	101238.5 ± 3543.4	116210 ± 4067.4
COD <sub>inert</sub> (mg/l)	31350 ± 1097.3	57000 ± 1995	82650 ± 2892.8
BOD <sub>5</sub> (mg/l)	64538 ± 2258.8	82065 ± 2872.3	99592 ± 3485.7
BOD <sub>5</sub> / COD <sub>dis</sub>	0.3 ± 0.011	0.6 ± 0.021	0.9 ± 0.032
Total N (mg/l)	193.4 ± 6.8	268.8 ± 9.41	344.2 ± 12.1
NH <sub>4</sub> -N (mg/l)	26.2 ± 0.92	33.8 ± 1.183	41.3 ± 1.5
NO <sub>3</sub> -N (mg/l)	44.5 ± 1.6	56.9 ± 1.992	69.2 ± 2.422
NO <sub>2</sub> -N (mg/l)	20.4 ± 0.714	24.9 ± 0.872	29.4 ± 1.03
Total P (mg/l)	497.1 ± 17.4	639.8 ± 22.393	782.4 ± 27.384
PO <sub>4</sub> -P (mg/l)	353.2 ± 12.362	460.2 ± 16.11	567.2 ± 19.9
<b>Polyphenols (mg/l)</b>			
catechol	3.1 ± 0.11	16.6 ± 0.6	30.1 ± 1.054
3-hydroxybenzoic acid	7.2 ± 0.252	19.7 ± 0.07	32.2 ± 1.13
tyrosol	7.1 ± 0.3	11.3 ± 0.4	15.4 ± 0.54
4-hydroxybenzoic acid	2.3 ± 0.081	9.2 ± 0.322	16.1 ± 0.564
4-hydroxyphenylacetic acid,	4.1 ± 0.144	6.2 ± 0.22	8.2 ± 0.3
3-hydroxyphenylpropionic acid	3.4 ± 0.12	4.3 ± 0.2	5.2 ± 0.182
4-hydroxyphenylpropionic acid	4.1 ± 0.144	6.1 ± 0.214	8.1 ± 0.284
3,4-dihydroxyphenylethanol	1.2 ± 0.042	3.2 ± 0.112	5.2 ± 0.182
3,4-dihydroxyphenylacetic acid.	0.6 ± 0.021	1.1 ± 0.04	1.6 ± 0.1
TAA (mg/l)	1240.2 ± 43.41	1906.3 ± 66.721	2572.4 ± 90.034
<b>Polyaromatics (mg/l)</b>			
aniline	43.3 ± 1.52	109.3 ± 3.83	175.2 ± 6.132
4-nitroaniline	50.2 ± 1.8	120.8 ± 4.23	191.3 ± 6.7
o-toluidine	28.0 ± 1.0	95.4 ± 3.34	162.8 ± 5.7
anisidine	49.1 ± 1.72	92.7 ± 3.3	136.2 ± 4.8
benzene	56 ± 1.96	63.6 ± 2.23	71.1 ± 2.5
nitrobenzene	33.1 ± 1.2	37.2 ± 1.302	41.3 ± 1.5
ethylbenzene	11.3 ± 0.4	51.2 ± 1.8	91.0 ± 3.2
3,6-bis(dimethylamino)durene	35.2 ± 1.232	79.7 ± 2.8	124.2 ± 4.4
benzidine	32.6 ± 1.141	66 ± 2.31	99.4 ± 3.5
dimethylalanine	21.1 ± 0.74	72.6 ± 2.541	124 ± 4.34
3,3-dichlorobenzidine	13.2 ± 0.462	24.2 ± 0.9	35.2 ± 1.232

**Table 3:** Characterization values of the OMW at pH=4.5 (n=3, mean values ± SD). (SD: standard deviation; n: the repeat number of experiments in this study).



### Preparation of Ni / Al<sub>2</sub>O<sub>3</sub> / TiO<sub>2</sub> Photocatalyst

An Al<sub>2</sub>O<sub>3</sub> (d<sub>50</sub> = 210 nm) powder was mixed with a TiO<sub>2</sub> (d<sub>50</sub> = 220 nm) powder by ball milling in deionized H<sub>2</sub>O for 24 h. NH<sub>3</sub> was added drop by drop into the slurry to reach a pH=9.2. A separate solution of the nickel nitrate [Ni(NO<sub>3</sub>)<sub>2</sub>•6H<sub>2</sub>O] was also prepared. The pH value of Ni(NO<sub>3</sub>)<sub>2</sub>•6H<sub>2</sub>O solution was also adjusted to 9.2. The Al<sub>2</sub>O<sub>3</sub> and TiO<sub>2</sub> slurry was poured into Ni(NO<sub>3</sub>)<sub>2</sub>•6H<sub>2</sub>O solution and then stirred for 30 min. The Ni+2 ion could then be absorbed onto the surface of Al<sub>2</sub>O<sub>3</sub> particles. The starting amounts of TiO<sub>2</sub> and Ni added into the slurry were adjusted to result in 5 vol% each to that of Al<sub>2</sub>O<sub>3</sub>. The resulting powder mixtures after coating were filtered, washed and dried. The powder mixtures were reduced in pure hydrogen at 550°C for 1 h, followed by ball milling in ethyl alcohol for 24 h with Al<sub>2</sub>O<sub>3</sub> grinding media. The Al<sub>2</sub>O<sub>3</sub> powder, Al<sub>2</sub>O<sub>3</sub>-TiO<sub>2</sub> and Al<sub>2</sub>O<sub>3</sub>-Ni powder mixtures were also prepared with the same technique.

5 g of TiO<sub>2</sub>, 5 g of Al<sub>2</sub>O<sub>3</sub> and 2g of Ni(NO<sub>3</sub>)<sub>2</sub>•6H<sub>2</sub>O were weighed, where the mass ratios of (1%/5%/10%; 10%/1%/5% and 1%/10%/5%), respectively. These three mixed raw materials with the designed proportion were grounded with an agate mortar for 30 min, and then sintered in a crucible under nitrogen gas [N<sub>2</sub>(g)] atmosphere at 400°C for 2 h, with the temperature rise rate of 20°C/1min. These samples were obtained after annealing and cooling down to the room temperature (at 25°C). The as-prepared composite was named according to the preparation conditions as illustrated by "Ni/Al<sub>2</sub>O<sub>3</sub>/TiO<sub>2</sub>". The mass ratios of Ni/Al<sub>2</sub>O<sub>3</sub>/TiO<sub>2</sub> were adjusted as 1%/5%/10%; 10%/1%/5% and 1%/10%/5%, respectively.

### Photocatalytic Degradation Reactor

A two liter cylinder kuvars glass reactor was used for the photodegradation experiments in the OMW under 500 W UV-vis and 50 W sun light irradiations, at different operational conditions. 1000 ml the OMW was filled for experimental studies and the photocatalyst were added to the cylinder glass reactor. The photocatalytic reaction was operated with constant stirring during the photocatalytic degradation process 500 W under UV-vis light and 50 W sun light irradiations. 10 ml of the reacting solution were sampled and centrifugated (at 10000 rpm) at different time intervals.

### Experimental Chemicals

Nano-Al<sub>2</sub>O<sub>3</sub>, nano-Ni(Ac)<sub>2</sub>, nano-TiO<sub>2</sub> and Ni(NO<sub>3</sub>)<sub>2</sub>•6H<sub>2</sub>O were purchased from Merck, (Germany). Helium, He(g) [gas chromatography (GC) grade, 99.98%] and N<sub>2</sub>(g) (GC grade, 99.98%) was purchased from Linde, (Germany). Catechol

(99%), 3-hydroxybenzoic acid (99%), tyrosol (99%), 4-hydroxybenzoic acid (99%), 4-hydroxyphenylacetic acid (99%), 3-hydroxyphenylpropionic acid (99%), 4-hydroxyphenylpropionic acid (99%), 3,4-dihydroxyphenylethanol, 3,4-dihydroxyphenylacetic acid (99%), aniline (99%), 4-nitroaniline (99%), o-toluidine (99%), anisidine (99%), benzene (99%), nitrobenzene (99%), ethylbenzene (99%), 3,6-bis(dimethylamino)durene (99%), benzidine (99%), dimethylaniline (99%) and 3,3-dichlorobenzidine (99%) were purchased from Aldrich, (Germany).

### Analytical Methods

pH, T(°C), oxydation reduction potential (ORP), DO, biochemical oxygen demand-5 days (BOD<sub>5</sub>), chemical oxygen demand-total (COD<sub>total</sub>), chemical oxygen demand-dissolved (COD<sub>dissolved</sub>), total suspended solids (TSS), total-nitrogen (Total-N), ammonia-nitrogen (NH<sub>3</sub>-N), nitrate-nitrogen (NO<sub>3</sub>-N), nitrite-nitrogen (NO<sub>2</sub>-N), total-phosphorus (Total-P) and phosphate-phosphorus (PO<sub>4</sub>-P) measurements were monitored following the Standard Methods 2310, 2320, 2550, 2580, 4500-O, 5210 B, 5220 D, 2540 D, 4500-N, 4500-NH<sub>3</sub>, 4500-NO<sub>3</sub>, 4500-NO<sub>2</sub> and 4500-P [31]. Inert COD or chemical oxygen demand-inert (COD<sub>inert</sub>) was measured according to glucose comparison method [32]. Aniline, 4-nitroaniline, o-toluidine, o-anisidine, benzene, nitrobenzene, ethylbenzene, 3,6-bis(dimethylamino)durene, benzidine, dimethylaniline and 3,3-dichlorobenzidine were identified as TAAs were identified with a high-pressure liquid chromatography (HPLC) (Agilent-1100) with a C-18 reverse phase HPLC column, (25 cm x 4.6 mm x 5 μm, (Ace5C-18). o-anisidine was measured in a HPLC (Agilent-1100) with a UV detector at a mobile phase of 35% acetonitrile / 65% H<sub>2</sub>O (water) at a flow rate of 1.2 ml/min.

Total phenol, catechol (99%), 3-hydroxybenzoic acid (99%), tyrosol (99%), 4-hydroxybenzoic acid (99%), 4-hydroxyphenylacetic acid (99%), 3-hydroxyphenylpropionic acid (99%), 4-hydroxyphenylpropionic acid (99%), 3,4-dihydroxyphenylethanol (99%) and 3,4-dihydroxyphenylacetic acid (99%) (HPLC, Agilent-1100) with a Spectra system model SN4000 pump and Asahipak ODP-506D column (150 cm x 6 mm x 5 μm).

500 W UV-vis light and 50 W sun light powers were used for the photocatalytic oxidation of the pollutant parameters in the OMW at different operational conditions such as at different mass ratios of Al<sub>2</sub>O<sub>3</sub>, TiO<sub>2</sub> and Ni (1%/5%/10%; 10%/1%/5% and 1%/10%/5%), at increasing photooxidation times (10, 30, 60, 100 and 120 min), at different Ni/Al<sub>2</sub>O<sub>3</sub>/TiO<sub>2</sub> photocatalyst concentrations (100, 250, 500, 750 and 1000 mg/l), pH values (3.5-4.0-7.0-10.0)

and temperatures (15°C, 25°C, 50°C and 75°C), under 500 W UV-vis and 50 W sun lights irradiations, respectively. Under the optimized conditions, the maximum COD<sub>dissolved</sub> total phenol and TAAs yields were 98%, 88%, 94%, respectively, at pH=9.0, at 500 mg/l Ni/Al<sub>2</sub>O<sub>3</sub>/TiO<sub>2</sub> NCs, under 500 W UV-vis light, after 100 min, at 50°C, respectively. The photodegradation yields in the OMW under sun light was lower than the photooxidation yields in the OMW under UV-vis light.

The detection limit (DL) of an individual analytical procedure is the lowest amount of analyte in one sample which can be detected but not necessarily quantitated as an exact value. The DL may be expressed as=3X standard deviation of low concentration / slope of the calibration line.

The quantification limit (QL) of an individual analytical procedure is the lowest amount of analyte in one sample which can be quantitatively determined with suitable precision and accuracy. The QL may be expressed as=10X standard deviation of low concentration / slope of the calibration line. All experiments were carried out three times and the results were given as the means of triplicate sampling with standard deviation (SD) values.

## Acute Toxicity Assays

### Microtox Acute Toxicity Test

Toxicity to the bioluminescent organism *Aliivibrio fischeri* (also called *Vibrio fischeri* or *V. fischeri*) was assayed using the Microtox measuring system according to DIN 38412L34, L341, (EPS 1/ RM/24 1992). Microtox testing was performed according to the standard procedure recommended by the manufacturer [33]. A specific strain of the marine bacterium, *V. fischeri-Microtox* LCK 491 kit was used for the Microtox acute toxicity assay. Dr. LANGE LUMIX-mini type luminometer was used for the microtox toxicity assay [34].

### Daphnia Magna Acute Toxicity Test

To test toxicity, 24-h born *Daphnia magna* were used as described in Standard Methods sections 8711A, 8711B, 8711C, 8711D and 8711E, respectively [35]. After preparing the test solution, experiments were carried out using 5 or 10 *Daphnia magna* introduced into the test vessels. These vessels had 100 ml of effective volume at 7.0– 8.0 pH, providing a minimum dissolved oxygen (DO) concentration of 6 mg/l at an ambient temperature of 20–25°C. Young *Daphnia magna* were used in the test ( $\leq 24$  h old); 24–48 h exposure is generally accepted as standard for a *Daphnia magna* acute toxicity test. The results were expressed as mortality percentage of the *Daphnia magna*. Immobile

animals were reported as dead *Daphnia magna*.

## Statistical Analysis

ANOVA analysis of variance between experimental data was performed to detect F and P values. The ANOVA test was used to test the differences between dependent and independent groups, [36]. Comparison between the actual variation of the experimental data averages and standard deviation is expressed in terms of F ratio. F is equal (found variation of the data averages/expected variation of the data averages). P reports the significance level, and d.f indicates the number of degrees of freedom. Regression analysis was applied to the experimental data in order to determine the regression coefficient  $R_2$ , [37]. The aforementioned test was performed using Microsoft Excel Program. All experiments were carried out three times and the results are given as the means of triplicate samplings. The data relevant to the individual pollutant parameters are given as the mean with standard deviation (SD) values.

## Results and Discussions

### Characterization Values of the OMW

The characterization values of raw OMW at pH=4.5 taken from the influent of a olive oil production industry in Izmir, Turkey is given in Table 3. This plant is operated with a three phase olive oil extraction process.

### Effect of Mass Ratios of Ni/Al<sub>2</sub>O<sub>3</sub>/TiO<sub>2</sub> on the OMW Pollutant Parameters

The photocatalytic performance of the synthesized catalyst sample which combined with three different Ni/Al<sub>2</sub>O<sub>3</sub>/TiO<sub>2</sub> mass ratios of (1%/5%/10%; 10%/1%/5% and 1%/10%/5%) (Table 4). The maximum photodegradation efficiency was obtained at 1%/10%/5% mass ratio of Ni/Al<sub>2</sub>O<sub>3</sub>/TiO<sub>2</sub> which is the maximum Ni can be act as photosensitizer, absorbing the UV-vis and sun lights (Table 4), which can inject the photogenerated electrons into TiO<sub>2</sub> conduction band as mentioned in the study performed by Tuan WH, et al. [38].

In other words, the interfacial behavior between Ni and TiO<sub>2</sub> may increase the photo-generated electron mobility in Al<sub>2</sub>O<sub>3</sub>. Meanwhile, the synergetic effect of the intrinsic properties of Ni and component in the present NCs is also beneficial for the electron transfer in the conduction band to reduce the pollutants (COD components, polyphenols and polyaromatics) in the OMW. Approximately similar photooxidation yields were obtained for Ni/Al<sub>2</sub>O<sub>3</sub>/TiO<sub>2</sub> mass ratios of 1%/5%/10% (the yields are very slightly lower than the removal efficiencies at 1%/10%/5% Ni/Al<sub>2</sub>O<sub>3</sub>/TiO<sub>2</sub>



mass ratio), since with high  $\text{TiO}_2$  mass ratio more electrons were activated by production of high  $\text{OH}^\bullet$  resulting in high pollutant photo-degradation in the OMW (Table 4). The effect of high Ni mass ratios in the  $\text{Ni}/\text{Al}_2\text{O}_3/\text{TiO}_2$  NCs formation (10%/1%/5%) was found to be not so significant. However, higher pollutant photodegradation yields were obtained for this Ni mass ratio (Table 4). The slightly lower photodegradation yields can be discussed as follows: The weakly bounded Ni on the stoichiometric  $\text{TiO}_2$  surface tend

to migrate and aggregate to form larger clusters on  $\text{Al}_2\text{O}_3$  [19].  $\text{TiO}_2$  is softer than  $\text{Al}_2\text{O}_3$ , so the hardness of samples always decreased with increases of  $\text{TiO}_2$  contents [39]. In this study, demonstrates that nanometer-sized Ni particles can be distributed uniformly onto the surface of  $\text{Al}_2\text{O}_3$  particles by employing a coating technique. As long as both  $\text{TiO}_2$  and Ni particles are incorporated simultaneously into  $\text{Al}_2\text{O}_3$  matrix, the coarsening of matrix grains is constrained.

Retention time (min)	$\text{Ni}/\text{Al}_2\text{O}_3/\text{TiO}_2$	Removal Efficiencies (%)							
		UV-vis light				Sun light			
		Parameters (mg/l)				Parameters (mg/l)			
		$\text{COD}_{\text{total}}$	$\text{COD}_{\text{dis}}$	Total phenol	TAAAs	$\text{COD}_{\text{total}}$	$\text{COD}_{\text{dis}}$	Total phenol	TAAAs
10	1%/5%/10%	48	47	48	50	43	39	42	48
	10%/1%/5%	42	40	36	52	42	37	34	46
	1%/10%/5%	53	50	57	67	52	49	55	65
30	1%/5%/10%	40	48	50	56	45	42	44	54
	10%/1%/5%	47	43	38	54	44	39	37	48
	1%/10%/5%	55	53	59	70	54	52	57	68
60	1%/5%/10%	54	53	56	62	49	51	54	60
	10%/1%/5%	51	49	45	65	48	47	42	63
	1%/10%/5%	70	68	65	86	68	65	63	84
100	1%/5%/10%	88	85	78	80	84	81	75	78
	10%/1%/5%	86	84	80	78	83	83	78	76
	1%/10%/5%	99	98	88	94	96	95	86	92
120	1%/5%/10%	84	83	75	76	81	79	73	74
	10%/1%/5%	82	79	71	77	79	76	70	73
	1%/10%/5%	95	93	84	92	94	92	81	90

**Table 4:** Effect of  $\text{Ni}/\text{Al}_2\text{O}_3/\text{TiO}_2$  mass ratios (1%/5%/10%, 10%/1%/5% and 1%/10%/5%) and retention times on the yields of the OMW during photocatalytic oxidation, at 500 mg/l  $\text{Ni}/\text{Al}_2\text{O}_3/\text{TiO}_2$  NCs, under 500 W UV-vis and 50 W sun lights, at pH=9.0 and at 50°C, after 100 min retention time, respectively.

### Establishment of the Optimum Retention Time for Photocatalytic Oxidations of the Pollutants in the OMW

The effects of increasing photooxidation retention times (10, 30, 60, 100 and 120 min) on the photocatalytic oxidation of pollutant parameters in the OMW, under 500 W UV-vis and 50 W sun lights, at 500 mg/l  $\text{Ni}/\text{Al}_2\text{O}_3/\text{TiO}_2$  NCs, at pH=9.0, at 50°C are shown in Table 4. The maximum  $\text{COD}_{\text{total}}$ ,  $\text{COD}_{\text{dis}}$ , polyphenols and polyaromatics yields in the OMW were 99%, 98%, 88% and 94%, respectively, under 500 W UV-

vis light, at 500 mg/l  $\text{Ni}/\text{Al}_2\text{O}_3/\text{TiO}_2$  NCs, at 1%/10%/5% mass ratio of  $\text{Ni}/\text{Al}_2\text{O}_3/\text{TiO}_2$ , at pH=9.0, at 50°C, after 100 min, respectively Table 4. The maximum  $\text{COD}_{\text{total}}$ ,  $\text{COD}_{\text{dis}}$ , total phenols and TAAAs yields in the OMW were 96%, 95%, 86% and 92%, respectively, under 50 W sun light, at 500 mg/l  $\text{Ni}/\text{Al}_2\text{O}_3/\text{TiO}_2$  NCs, at 1%/10%/5% mass ratio of  $\text{Ni}/\text{Al}_2\text{O}_3/\text{TiO}_2$ , at pH=9.0, at 50°C, after 100 min, respectively Table 4. As the photo-oxidation times were increased from 10 min up to 60 min in the presence of 500 mg/l  $\text{Ni}/\text{Al}_2\text{O}_3/\text{TiO}_2$  NCs, the photooxidation yields were increased in all pollutant parameters in the OMW under 500 W UV-vis light (Table 4).

Similarly, the removal efficiencies increased as the contact time between pollutants and 500 mg/l Ni/Al<sub>2</sub>O<sub>3</sub>/TiO<sub>2</sub> NCs posite increased from 10 min to 60 min in the OMW, under 50 W sun light. On the other hand, the removal efficiencies of pollutant parameters in the OMW slightly decreased in the same UV-vis and sun lighths as the increasing retention times from 100 to 120 min, respectively (Table 4). Low contact times cannot be enough for OH● production throughout photooxidation process while high contact times can be decompose the structure and the pores of Ni/Al<sub>2</sub>O<sub>3</sub>/TiO<sub>2</sub> NCs, and the photocatalysts may to covered completely with the particles of pollutant parameters (COD<sub>total</sub>, COD<sub>dis</sub>, total phenols and TAAs). Therefore, it was that the maximum removal efficiencies were observed at 100 min retention time during experimental studies Table 4.

### Effect of Different Ni/Al<sub>2</sub>O<sub>3</sub>/TiO<sub>2</sub> NCs Concentrations on the Photocatalytic Oxidation of the Pollutants in the OMW

Since the maximum photooxidation removals of Ni/Al<sub>2</sub>O<sub>3</sub>/TiO<sub>2</sub> NCs was obtained with mass ratio of 1%/10%/5% the studies performed with this form of the nanocomposite synthesized under laboratory conditions. The rate of photocatalytic reaction and the removals of pollutants in the OMW are strongly influenced by the amount of the photocatalyst. Heterogeneous photocatalytic reactions are known to show proportional increase in photooxidation with catalyst loading. Generally, in any given photocatalytic application, the optimum catalyst concentration must be determined in order to avoid excess usage of catalyst and to ensure the total absorption of efficient photons.

As shown in Table 5, four different Ni/Al<sub>2</sub>O<sub>3</sub>/TiO<sub>2</sub> NCs concentrations (50, 250, 500 and 1000 mg/l) were used to determine the maximum yields of pollutant parameters {COD components [COD<sub>total</sub>, COD<sub>dis</sub>, COD<sub>inert</sub>, respectively], polyphenols [catechol, 3-hydroxybenzoic acid, tyrosol, 4-hydroxybenzoic acid, 4-hydroxyphenylacetic acid, 3-hydroxyphenylpropionic acid, 4-hydroxyphenylpropionic acid, 3,4-dihydroxyphenylethanol, 3,4-dihydroxyphenylacetic acid, respectively], TAAs metabolites [aniline, 4-nitroaniline, o-toluidine, o-anisidine, benzene, nitrobenzene, ethylbenzene, 3,6-bis(dimethylamino)durene, benzidine, dimethylaniline, 3,3-dichlorobenzidine, respectively]} in the OMW throughout photocatalytic oxidation, under UV-vis and sun lighths. The maximum COD<sub>total</sub>, COD<sub>dis</sub> and

COD<sub>inert</sub> removal efficiencies in the OMW were 99%, 98% and 73%, respectively, under 500 W UV-vis light, at 500 mg/l Ni/Al<sub>2</sub>O<sub>3</sub>/TiO<sub>2</sub> NCs, at 1%/10%/5% mass ratio of Ni/Al<sub>2</sub>O<sub>3</sub>/TiO<sub>2</sub>, at pH=9.0, at 50°C, after 100 min, respectively Table 5. The maximum removal efficiencies of total phenols and polyphenols; such as, catechol, 3-hydroxybenzoic acid, tyrosol, 4-hydroxybenzoic acid, 4-hydroxyphenylacetic acid, 3-hydroxyphenylpropionic acid, 4-hydroxyphenylpropionic acid, 3,4-dihydroxyphenylethanol, 3,4-dihydroxyphenylacetic acid in the OMW were 88%, 87%, 86%, 88%, 83%, 86%, 85%, 88%, 88% and 87%, respectively, under 500 W UV-vis light, at 500 mg/l Ni/Al<sub>2</sub>O<sub>3</sub>/TiO<sub>2</sub> NCs, at 1%/10%/5% mass ratio of Ni/Al<sub>2</sub>O<sub>3</sub>/TiO<sub>2</sub>, at pH=9.0, at 50°C, after 100 min, respectively Table 5.

The maximum removal efficiencies of TAAs and TAAs metabolites; such as, aniline, 4-nitroaniline, o-toluidine, o-anisidine, benzene, nitrobenzene, ethylbenzene, 3,6-bis(dimethylamino)durene, benzidine, dimethylaniline, 3,3-dichlorobenzidine in the OMW were 94%, 92%, 90%, 91%, 89%, 88%, 93%, 92%, 85%, 93%, 89% and 90%, respectively, under 500 W UV-vis light, at 500 mg/l Ni/Al<sub>2</sub>O<sub>3</sub>/TiO<sub>2</sub> NCs, at 1%/10%/5% mass ratio of Ni/Al<sub>2</sub>O<sub>3</sub>/TiO<sub>2</sub>, at pH=9.0, at 50°C, after 100 min, respectively Table 5. On the other hand, the pollutant parameters (COD components, polyphenols and TAAs metabolites) removal efficiencies were increased from 50 to 250 mg/l Ni/Al<sub>2</sub>O<sub>3</sub>/TiO<sub>2</sub> NCs concentrations under 500 W UV-vis light. Therefore, the removal efficiencies of the pollutant parameters (COD components, polyphenols and TAAs metabolites) were slightly decreased from 500 to 1000 mg/l Ni/Al<sub>2</sub>O<sub>3</sub>/TiO<sub>2</sub> NCs concentrations under 500 W UV-vis light Table 5. The observation was that removal efficiency increased as the quantity of the nanocomposite was increased. However, in this study low photooxidation removals was observed with low (50 mg/l) and high (1000 mg/l) Ni/Al<sub>2</sub>O<sub>3</sub>/TiO<sub>2</sub> concentrations. The inhibition effect of over loaded photocatalysts concentrations for the pollutant parameter removals in the OMW was detected. Probably the structural decomposition of photocatalysts, the pore surfaces of photocatalysts may to cover completely with the particles of pollutant parameters (COD<sub>total</sub>, COD<sub>dis</sub>, total phenols and TAAs) or other radical species [carbon based radicals such as carboxyl radicals (CO<sub>2</sub>●)]. The effect of photocatalyst quantity can be explained by the fact that decreasing the amount of photocatalyst decreases the number of activities on the Ni-TiO<sub>2</sub> surface, which in turn in decreases the numbers of hy OH● and hydroperoxyl (OH<sub>2</sub>●) radicals.

Parameters (mg/l)	Removal Efficiencies (%)							
	UV-vis light				Sun light			
	Ni/Al <sub>2</sub> O <sub>3</sub> /TiO <sub>2</sub> NCs (mg/l)				Ni/Al <sub>2</sub> O <sub>3</sub> /TiO <sub>2</sub> NCs (mg/l)			
	100	250	500	1000	100	250	500	1000
COD <sub>total</sub>	57	72	99	94	56	70	96	92
COD <sub>dissolved</sub>	56	70	98	93	54	67	95	91
COD <sub>inert</sub>	39	48	73	65	37	46	70	61
Total phenol	62	68	88	87	60	65	86	84
<b>Polyphenols</b>								
catechol	60	67	87	86	58	64	86	83
3-hydroxybenzoic acid	57	66	86	84	53	65	85	83
tyrosol	59	64	88	86	56	61	86	84
4-hydroxybenzoic acid	57	68	83	78	53	60	82	75
4-hydroxyphenylacetic acid,	55	66	86	79	52	64	84	72
3-hydroxyphenylpropionic acid	57	63	85	83	55	61	83	78
4-hydroxyphenylpropionic acid	51	64	88	81	49	63	86	80
3,4-dihydroxyphenylethanol	58	65	88	85	54	62	86	82
3,4-dihydroxyphenylacetic acid.	61	67	87	84	59	65	85	82
TAAAs	73	89	94	93	70	86	92	91
<b>Polyaromatics</b>								
Aniline	53	64	92	84	51	61	90	81
4-nitroaniline	58	63	90	82	57	60	88	79
o-toluidine	59	67	91	81	58	65	90	77
o-anisidine	48	65	89	88	46	63	87	86
benzene	49	65	88	82	47	60	87	79
nitrobenzene	56	67	93	90	55	64	91	88
ethylbenzene	50	62	92	78	48	59	91	75
3,6-bis(dimethylamino)durene	54	65	85	78	50	62	84	76
benzidine	46	67	93	75	43	60	92	72
dimethylalanine	57	70	89	76	54	65	87	71
3,3-dichlorobenzidine	43	74	90	70	41	59	88	68

**Table 5:** Effect of increasing Ni/Al<sub>2</sub>O<sub>3</sub>/TiO<sub>2</sub> NCs concentrations during photocatalytic oxidation on the yields of OMW, under 500 W UV-vis and 50 W sun lights, at 1%/10%/5% mass ratio of Ni/Al<sub>2</sub>O<sub>3</sub>/TiO<sub>2</sub>, at pH=9.0, at 50°C, after 100 min, respectively.

The maximum COD<sub>total</sub>, COD<sub>dis</sub> and COD<sub>inert</sub> removal efficiencies in the OMW were 96%, 95% and 70%, respectively, under 50 W sun light, at 500 mg/l Ni/Al<sub>2</sub>O<sub>3</sub>/ZrO<sub>2</sub> NCs, at 1%/10%/5% mass ratio of Ni/Al<sub>2</sub>O<sub>3</sub>/TiO<sub>2</sub>, at pH=9.0, at 50°C, after 100 min, respectively (Table 5). The maximum removal efficiencies of total phenols and polyphenols; such as, catechol, 3-hydroxybenzoic acid, tyrosol, 4-hydroxybenzoic acid, 4-hydroxyphenylacetic acid, 3-hydroxyphenylpropionic acid, 4-hydroxyphenylpropionic acid, 3,4-dihydroxyphenylethanol, 3,4-dihydroxyphenylacetic

acid in the OMW were 86%, 85%, 86%, 82%, 84%, 83%, 86%, 86% and 85%, respectively, under 50 W sun light, at 500 mg/l Ni/Al<sub>2</sub>O<sub>3</sub>/TiO<sub>2</sub> NCs, at 1%/10%/5% mass ratio of Ni/Al<sub>2</sub>O<sub>3</sub>/TiO<sub>2</sub>, at pH=9.0, at 50°C, after 100 min, respectively (Table 5). The maximum removal efficiencies of TAAAs and TAAAs metabolites; such as, aniline, 4-nitroaniline, o-toluidine, o-anisidine, benzene, nitrobenzene, ethylbenzene, 3,6-bis(dimethylamino)durene, benzidine, dimethylalanine, 3,3-dichlorobenzidine in the OMW were 90%, 88%, 90%, 87%, 87%, 91%, 91%, 84%, 92%, 87% and 88%, respectively,

under 50 W sun light, at 500 mg/l Ni/Al<sub>2</sub>O<sub>3</sub>/TiO<sub>2</sub> NCs, at 1%/10%/5% mass ratio of Ni/Al<sub>2</sub>O<sub>3</sub>/TiO<sub>2</sub>, at pH=9.0, at 50°C, after 100 min, respectively (Table 5). The result of the photocatalytic oxidation yields of the pollutant parameters in the OMW with Ni/Al<sub>2</sub>O<sub>3</sub>/TiO<sub>2</sub> under sun light showed that the yields were slightly lower than the photocatalytic oxidation yields of the pollutant parameters in the OMW under UV-vis light. In addition to, the pollutant parameters (COD components, polyphenols and TAAs metabolites) removal efficiencies were increased from 50 to 250 mg/l Ni/Al<sub>2</sub>O<sub>3</sub>/TiO<sub>2</sub> NCs concentrations under 50 W sunlight. However, the removal efficiencies of the pollutant parameters (COD components, polyphenols and TAAs metabolites) were slightly decreased from 500 to 1000 mg/l Ni/Al<sub>2</sub>O<sub>3</sub>/TiO<sub>2</sub> NCs concentrations under 50 W sun light Table 5.

Tuan WH, et al. [38] reported to the dense Al<sub>2</sub>O<sub>3</sub>/(TiO<sub>2</sub> + Ni) NCs are prepared by pulse electric current sintering (PECS) at 1350°C for 5 min or by pressureless sintering (PLS) at 1600°C for 60 min. The sub-micrometer-sized TiO<sub>2</sub> particle acts as microstructural stabilizer that slows down the coarsening of matrix grains in the composites prepared by both processes. Due to microstructural refinement, the strength of the Al<sub>2</sub>O<sub>3</sub>/(5%TiO<sub>2</sub> + 1%Ni) nanocomposite is ≈ 40% higher than that of Al<sub>2</sub>O<sub>3</sub> alone [38].

### Establishment of Optimum Temperature Value for Photocatalytic Oxidation of the OMW Pollutants with Ni/Al<sub>2</sub>O<sub>3</sub>/TiO<sub>2</sub>

The effects of increasing temperature values (15, 25, 50 and 80°C) on the photocatalytic oxidation of the OMW pollutants was investigated, under 500 W UV-vis and 50 W sun lights, at optimum photocatalyst concentration (500 mg/l Ni/Al<sub>2</sub>O<sub>3</sub>/TiO<sub>2</sub> NCs), at optimum pH value (pH=9.0), at optimum retention time (100 min). The increasing of temperature values from 15 to 25°C showed a raise in the removal efficiencies of OMW pollutants in both UV-vis conditions. The maximum COD<sub>total</sub>, COD<sub>dis'</sub> total phenols and TAAs removal efficiencies in the OMW were 99%, 98%, 88% and 94%, respectively, under 500 W UV-vis light, at pH=9.0, at 50°C, after 100 min, respectively Table 6. The removal efficiencies of COD<sub>total</sub>, COD<sub>dis'</sub> total phenols and TAAs in the OMW were 96%, 95%, 86% and 92%, respectively, under 50 W sun light, at 500 mg/l Ni/Al<sub>2</sub>O<sub>3</sub>/TiO<sub>2</sub> NCs, at 1%/10%/5% mass ratio of Ni/Al<sub>2</sub>O<sub>3</sub>/TiO<sub>2</sub>, at pH=9.0, at 50°C, after 100 min, respectively Table 6. The photocatalytic oxidation yields of the pollutant parameters slightly decreased as the temperature increased from 50 to 80°C in both types of irradiation lights Table 6. Therefore, the optimum operational temperature was selected as 50°C for the maximum removals of pollutant parameters in the OMW during photocatalytic oxidation.

Parameters (mg/l)	Removal efficiencies (%)							
	UV-vis light				Sun light			
	T(°C)				T(°C)			
	15	25	50	80	15	25	50	80
COD <sub>total</sub>	80	98	99	82	79	95	96	81
COD <sub>dissolved</sub>	78	97	98	81	76	94	95	74
COD <sub>inert</sub>	69	72	73	65	67	69	70	62
Total phenol	84	86	88	79	82	84	86	75
<b>Polyphenols</b>								
catechol	79	80	87	83	66	74	86	80
3-hydroxybenzoic acid	81	83	86	85	74	77	85	77
tyrosol	83	84	88	87	80	82	86	81
4-hydroxybenzoic acid	78	77	83	79	74	76	82	74
4-hydroxyphenylacetic acid	71	78	86	84	65	76	84	79
3-hydroxyphenylpropionic acid	79	84	85	78	76	82	83	74
4-hydroxyphenylpropionic acid	77	85	88	87	76	83	86	80
3,4-dihydroxyphenylethanol	74	84	88	79	71	80	86	71
3,4-dihydroxyphenylacetic acid.	79	86	87	86	76	79	85	84
TAAs	89	90	94	86	85	89	92	79

Polyaromatics								
aniline	80	85	92	87	76	83	90	75
4-nitroaniline	76	87	90	85	74	85	88	79
o-toluidine	75	82	91	84	73	81	90	74
anisidine	82	91	89	92	78	90	87	83
benzene	84	85	88	87	80	82	87	86
nitrobenzene	80	86	93	90	77	81	91	89
ethylbenzene	72	88	92	89	69	85	91	87
3,6-bis(dimethylamino)durene	70	76	85	78	62	75	84	76
benzidine	73	75	93	91	70	74	92	89
dimethylalanine	68	72	89	86	60	69	87	84
3,3-dichlorobenzidine	65	74	90	87	64	67	88	85

**Table 6:** Effect of increasing temperature values during photocatalytic oxidation on the yields of OMW, under 500 W UV-vis and 50 W sun lights, at 500 mg/l Ni/Al<sub>2</sub>O<sub>3</sub>/TiO<sub>2</sub> NCs, at 1%/10%/5% mass ratio of Ni/Al<sub>2</sub>O<sub>3</sub>/TiO<sub>2</sub>, at pH=9.0, after 100 min, respectively.

### Establishment of the Optimum pH Value for Photocatalytic Oxidation in the OMW

Table 7 shows the effect of increasing pH values (4.0-7.0-9.0-10.0) throughout photocatalytic oxidation on the yields of the OMW, under 500 W UV-vis and 50 W sun lights, at optimum retention time (100 min), at room temperature (25°C), at optimum photocatalyst concentration (500 mg/l Ni/Al<sub>2</sub>O<sub>3</sub>/TiO<sub>2</sub> NCs). The maximum COD<sub>total</sub>, COD<sub>dis</sub>, total phenols and TAAs removal efficiencies in the OMW were 99%, 98%, 88% and 94%, respectively, under 500 W UV-vis, at 500 mg/l Ni/Al<sub>2</sub>O<sub>3</sub>/TiO<sub>2</sub> NCs, at pH=9.0, at 50°C, after 100 min, respectively Table 7. In addition to, COD<sub>total</sub>, COD<sub>dis</sub>, total phenols and TAAs removal efficiencies in the OMW were 96%, 95%, 86% and 92%, respectively, under 50 W sun light, at 500 mg/l Ni/Al<sub>2</sub>O<sub>3</sub>/TiO<sub>2</sub> NCs, at pH=9.0, at 50°C, after 100 min, respectively Table 7. The photooxidation removal efficiencies decreased as the pH was decreased from 7.0 to 4.0 and increased from 7.0 up to 9.0 and up to 10.0 under both UV-vis and sun lights, at 500 mg/l Ni/Al<sub>2</sub>O<sub>3</sub>/TiO<sub>2</sub> NCs, at 1%/10%/5% mass ratio of Ni/Al<sub>2</sub>O<sub>3</sub>/TiO<sub>2</sub>, at 50°C, after

100 min, respectively Table 7. This phenomenon may be attributed to the fact that as pH is neutral, the concentration of OH ions also increases, thus causing Ni-TiO<sub>2</sub> to generate OH<sup>-</sup> and O<sup>2-</sup> more efficiently. However, it is also seen that the rate of removal diminished for the values beyond pH=7.0. This is possibly because at higher pH values, the negatively charged photocatalyst surface repulses the pollutant anions, thereby reducing the all pollutant efficiencies in the OMW. The lower photooxidation rate of the phenolic and aromatic compounds at pH=10.0 is likely a result of the low adsorption onto the surfaces of Ni/Al<sub>2</sub>O<sub>3</sub>/TiO<sub>2</sub> NCs. Another explanation regarding the languor of the process at high pH levels is the presence of carbonate (CO<sub>3,2-</sub>) ions, which could scavenge the OH●, or holes produced on the activated TiO<sub>2</sub> surface, comprising a less reactive carbonate (CO<sub>3</sub>●) radical, slowing the degradation and mineralization process. Samples prepared at neutral pH exhibit more surface area and higher reactivity than those prepared at lower and higher pH. Photocatalytic oxidation process for optimum operational conditions were explained.



Parameters (mg/l)	Removal efficiencies (%)							
	UV-vis light				Sun light			
	pH values				pH values			
	4	7	9	10	4	7	9	10
COD <sub>total</sub>	69	82	99	98	66	80	96	95
COD <sub>dissolved</sub>	66	80	98	97	62	77	95	94
COD <sub>inert</sub>	56	69	73	71	53	68	70	69
Total phenol	65	86	88	88	60	83	86	84
<b>Polyphenols</b>								
catechol	87	81	87	85	75	75	86	82
3-hydroxybenzoic acid	85	83	86	86	80	76	85	84
tyrosol	89	85	88	87	79	76	86	81
4-hydroxybenzoic acid	82	80	83	82	79	78	82	80
4-hydroxyphenylacetic acid	86	83	86	85	80	74	84	81
3-hydroxyphenylpropionic acid	85	81	85	82	79	77	83	80
4-hydroxyphenylpropionic acid	85	79	88	84	83	78	86	82
3,4-dihydroxyphenylethanol	88	81	88	83	80	76	86	79
3,4-dihydroxyphenylacetic acid.	86	78	87	84	77	75	85	80
TAAAs	68	90	94	93	66	86	92	89
<b>Polyaromatics</b>								
aniline	66	80	92	86	60	76	90	83
4-nitroaniline	65	78	90	83	61	75	88	81
o-toluidine	62	76	91	84	59	74	90	80
anisidine	49	83	89	91	45	79	87	88
benzene	50	85	88	93	48	81	87	89
nitrobenzene	60	82	93	90	57	78	91	89
ethylbenzene	64	73	92	78	62	70	91	74
3,6-bis(dimethylamino)durene	78	68	85	76	72	66	84	72
benzidine	85	71	93	82	83	67	92	75
dimethylalanine	86	70	89	85	84	69	87	72
3,3-dichlorobenzidine	82	68	90	81	80	61	88	74

**Table 7:** Effect of increasing pH values on the yields of OMW during photocatalytic oxidation, under 500 W UV-vis and 50 W sun lights, at 500 mg/l Ni/Al<sub>2</sub>O<sub>3</sub>/TiO<sub>2</sub> NCs, at 1%/10%/5% mass ratio of Ni/Al<sub>2</sub>O<sub>3</sub>/TiO<sub>2</sub>, at 50°C, after 100 min, respectively.

### Photocatalytic Reaction Mechanism

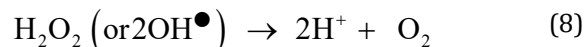
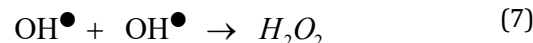
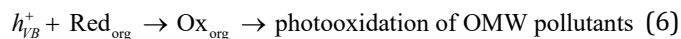
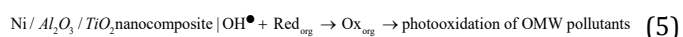
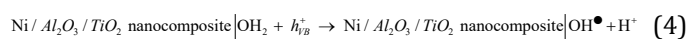
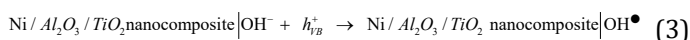
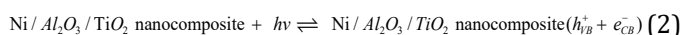
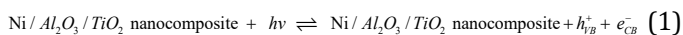
A photocatalytic reaction, in general, consists of three steps [39]. First, photocatalysis is initiated by bombarding a photocatalyst with UV light photons. Second, suppose the photon energy is greater than the band gap. In that case, these photons cause the generation of electrons (e<sup>-</sup>) on the surface of the photocatalyst to become 'excited' in the valence band (VB), causing them to move to the conduction band (CB). Simultaneously, a positive hole (h<sup>+</sup>VB) is formed on the VB.

Electrons and holes are excited and migrate to the surface of photocatalysts, where they react with adsorbed electron acceptors and donors, respectively [39]. Today, as in previous years, the use of bare TiO<sub>2</sub> nanomaterials and TiO<sub>2</sub> doped with other nanomaterials; It attracts great attention due to its potential applications in eliminating environmental pollution [40]. Nevertheless, due to its relatively large band gap energy (3.2 eV and 3.0 V for anatase and rutile phases, respectively), it can only absorb approximately 6% of the solar energy that reaches the earth at any given time. Thus, significant effort

has been devoted to enhancing  $\text{TiO}_2$ 's absorption properties in the visible spectrum and developing new photocatalytic materials that can capture a broad range, from UV to visible light and even the near-infrared region [39]. This strategy will lead to even more efficient use of solar energy, a clean, abundant and renewable energy source. Photocatalysts are nanomaterials whose surface modification, modification and structure design can be optimized to enhance and extend light absorption.

### Photooxidation Mechanisms of $\text{Ni}/\text{Al}_2\text{O}_3/\text{TiO}_2$ NCs

Overall, the mechanism of photocatalysis can be divided into five steps: (1) transfer of reactants in the fluid phase to the surface; (2) adsorption of the reactants; (3) reaction in the adsorbed phase; (4) desorption of the products; and (5) removal of products from the interface region [41,42]. A photocatalyst is a substance that, after being irradiated by light, can induce a chemical reaction in such a way that the actual substance of the catalyst will not be consumed [43]. It is well known that the photocatalytic activity could be controlled by varieties of factors such as surface area, phase structure, interfacial charge transfer, and separation efficiency of photo-induced electrons and holes. In this work, Ni molecule which acted as an electron shuttle was mostly in contact with the surface of  $\text{Al}_2\text{O}_3/\text{TiO}_2$  composite so that it could effectively transfer the photoelectrons from conduction band of  $\text{Al}_2\text{O}_3/\text{TiO}_2$  composite after being illuminated under UV light irradiation. Therefore, the photo-generated electrons in the  $\text{Ni}/\text{Al}_2\text{O}_3/\text{TiO}_2$  photocatalyst could easily migrate from the inner region to the surface to take part in the surface reaction. Such series this photocatalysts can be easily recycled from the aqueous solution because of the soft magnetism feature of combined Ni particles. The photocatalytic performance and the enhanced photocatalytic mechanism occurred on the interface of  $\text{Ni}-\text{TiO}_2$  [34]. The mechanism of photooxidation of polyphenols, COD and TAAs on  $\text{Ni}/\text{Al}_2\text{O}_3/\text{TiO}_2$  NCs surface was as follows: The excitation of  $\text{Ni}/\text{Al}_2\text{O}_3/\text{TiO}_2$  NCs by solar energy leads to the formation of an electron-hole pair. The hole combines with  $\text{H}_2\text{O}$  to form  $\text{OH}^\bullet$  while electron converts  $\text{O}_2(\text{g})$  to superoxide radical ( $\text{O}_2^{\bullet-}$ ), a strong oxidizing species as shown below (Equations 1, 2, 3, 4, 5, 6, 7 and 8):



COD, polyphenols and TAAs are degraded via photo-oxidation process by reacting with both  $\text{OH}^\bullet$  and  $h\nu$  [according to Eqs (1)  $\rightarrow$  (2), (3)  $\rightarrow$  (4) and (1)  $\rightarrow$  (5)]. The  $\text{OH}^\bullet$  shows electrophilic character and prefers to attack electron rich ortho or para carbon atoms of COD, polyphenols and TAAs. This results in the formation of polyphenol metabolites (catechol, 3-hydroxybenzoic acid, tyrosol, 4-hydroxybenzoic acid, 4-hydroxyphenylacetic acid, 3-hydroxyphenylpropionic acid, 4-hydroxyphenylpropionic acid, 3,4-dihydroxyphenylethanol, 3,4-dihydroxyphenylacetic acid) from total phenol and TAAs metabolites [aniline, 4-nitroaniline, o-toluidine, o-anisidine, benzene, nitrobenzene, ethylbenzene, 3,6-bis(dimethylamino)durene, benzidine, dimethylaniline, 3,3-dichlorobenzidine] from TAAs are formed with photooxidation process in the OMW under UV-vis and sun light irradiation, respectively. Radicals that undergo further reaction with DO in the OMW to yield polyphenols by-products (catechol, 3-hydroxybenzoic acid, tyrosol, 4-hydroxybenzoic acid, 4-hydroxyphenylacetic acid, 3-hydroxyphenylpropionic acid, 4-hydroxyphenylpropionic acid, 3,4-dihydroxyphenylethanol, 3,4-dihydroxyphenylacetic acid), and polyaromatics metabolites [aniline, 4-nitroaniline, o-toluidine, o-anisidine, benzene, nitrobenzene, ethylbenzene, 3,6-bis(dimethylamino)durene, benzidine, dimethylaniline, 3,3-dichlorobenzidine], respectively, with simultaneous generation of hydrogen peroxide ( $\text{H}_2\text{O}_2$ ) and (oxygen radicals ( $\text{O}_2^\bullet$ )). The  $\text{O}_2^\bullet$  produces  $\text{H}_2\text{O}_2$  and  $\text{O}_2$  again by disproportion, and generation of  $\text{OH}^\bullet$  accompanied with the production and consumption of  $\text{H}_2\text{O}_2$ .

Tuan WH et al. [38] also demonstrates that nanometer-sized Ni particles can be distributed uniformly onto the surface of  $\text{Al}_2\text{O}_3$  particles by employing a coating technique. As long as both  $\text{TiO}_2$  and Ni particles are incorporated simultaneously into  $\text{Al}_2\text{O}_3$  matrix, the coarsening of matrix grains is constrained. Due to the coarsening during sintering is limited by the addition of the inclusions; the nanocomposite can also be prepared by pressureless sintering.

The applications of ceramics as structural components are restricted because of their poor mechanical performance. To improve the mechanical properties of ceramics has thus attracted much attention. One of the most promising approaches is incorporating second-phase reinforcement into ceramic matrix [44]. The second-phase reinforcement

can be either a ceramic or a metallic phase. The presence of the second-phase inclusions can prohibit the propagation of crack and thus enhance the toughness of ceramics.

Yang et al. [41] investigated by the influences of TiO<sub>2</sub> NPs on the mechanical properties and microstructure of hot-pressing cerium-tetragonal zirconia polycrystal (TZP) based aluminium trioxide [Ce-TZP/Al<sub>2</sub>O<sub>3</sub>] ceramics were investigated. Meanwhile, t-TiO<sub>2</sub> to m-TiO<sub>2</sub> transformation toughening mechanism was investigated by X-ray diffractometry (XRD) method, the results show that when the percentage of TiO<sub>2</sub> was 20%, the mechanical properties and microstructures of materials are optimum. Moreover, transmission electron microscopy (TEM) observation show dislocation structures formation both in the Al<sub>2</sub>O<sub>3</sub> and on the grain boundary [41].

Mechanisms of polyphenols by products: Pyrolysis differs from other high-temperature processes like combustion and hydrolysis in that it does not involve reactions with O<sub>2</sub>, H<sub>2</sub>O or any other reagents. Pyrolysis of organic substances produces gas and liquid products and leaves a solid residue richer in carbon content. Pyrolytic destruction of phenol in the gas phase is negligible; the degradation occurs mainly in the bulk solution. A possible explanation for this is that a considerable increase in the concentration results in the formation of a complex H-bonding network between the phenolic compounds. It is well known that molecules containing carboxyl or carbohydrates (COOH or CHO) groups exist as dimers in solution due to the formation of H-bonds between two neighbouring molecules. This results in a more robust and stable configuration, thus leading to reduced degradation [45]. At this study, the major phenolic compounds in OMW after photocatalytic oxidation process reported by [46,47] and [48] as shown in Table 3. Benzene, tyrosol, caffeic acid...etc. (major aromatic amines) in OMW [49] during the photooxidation process of polyphenols.

### Mechanisms of Polyaromatics Metabolites

Hydrolysis and pyrolysis are main degradation mechanisms for aromatic amines with photooxidation. The attack of non-volatile compounds in the "bulk" water by OHL that destroy the chromophoric system through azo bond cleavage. OHL attack leads to hydroxyl amines followed by subsequent oxidation forming aromatic nitroso and nitro compounds. The attack at the carbon atom adjacent to the azo bond, leading to phenyl derivative radicals. Further degradation pathways are difficult to predict since the fate of the fragments depends on their physical and chemical properties. Further reactions may occur inside the cavity (pyrolysis), in the hypercritical water layer or in the 1616bulk water [49]. In the present study, the major aromatic amines in the OMW after photooxidation process

reported by [49] as seen in Table 3. Benzene (major aromatic amines) in the OMW [49] during the photooxidation process of polyaromatics.

### Acute Toxicity Assays

#### Effect of Ni/Al<sub>2</sub>O<sub>3</sub>/TiO<sub>2</sub> NCs Concentrations on the Microtox Acute Toxicity Removal Efficiencies in OMW at Increasing Photo-oxidation Time and Temperature

In Microtox with *Aliivibrio fischeri* (also called *Vibrio fischeri*) acute toxicity test, the initial EC<sub>90</sub> values at pH=7.0 was found as 100000 mg/l at 25°C Table 8, SET 1. The regression equation and regression coefficient of raw OMW, (control or blank sample) for EC<sub>90</sub>=100000 mg/l was calculated to  $y=0.0018x-90.942$ ,  $R_2=0.9890$ , at pH=7.0 and 25°C. After 60 min, 120 and 150 min of photocatalytic oxidation the EC<sub>90</sub> values decreased to EC<sub>40</sub>=60316 mg/l to EC<sub>15</sub>=37802 mg/l and to EC<sub>10</sub>=23804 mg/l in Ni/Al<sub>2</sub>O<sub>3</sub>/TiO<sub>2</sub> NCs=500 mg/l at 30°C Table 8, SET 3. The toxicity removal efficiencies were 55.56%, 83.33% and 88.89% after 60 min, 120 min and 150 min photocatalytic oxidation times, respectively, in Ni/Al<sub>2</sub>O<sub>3</sub>/TiO<sub>2</sub> NCs=500 mg/l at 30°C Table 8, SET 3.

The EC<sub>90</sub> values decreased to EC<sub>35</sub>, to EC<sub>10</sub> and to EC<sub>5</sub> after 60 min, 120 min and 150 min photocatalytic oxidation times, respectively, in Ni/Al<sub>2</sub>O<sub>3</sub>/TiO<sub>2</sub> NCs=500 mg/l at 60°C Table 8, SET 3. The EC<sub>35</sub>, the EC<sub>10</sub> and the EC<sub>5</sub> values were measured as 75000 mg/l, 62000 and 58000 mg/l, respectively, in Ni/Al<sub>2</sub>O<sub>3</sub>/TiO<sub>2</sub> NCs=500 mg/l at 60°C. The toxicity removal efficiencies were 61.11%, 88.89% and 94.44% after 60 min, 120 min and 150 min photocatalytic oxidation times, respectively, in Ni/Al<sub>2</sub>O<sub>3</sub>/TiO<sub>2</sub> NCs=500 mg/l at 60°C Table 8, SET 3. 94.44% maximum Microtox acute toxicity yield was found in Ni/Al<sub>2</sub>O<sub>3</sub>/TiO<sub>2</sub> NCs=500 mg/l after 150 min photocatalytic oxidation time at 60°C (Table 8, SET 3).

The regression equation and regression coefficient of EC<sub>35</sub>=75000 mg/l was measured to  $y=0.0005x+20.724$ ,  $R_2=0.9956$ , after 60 min photocatalytic oxidation time, at pH=7.0 and 60°C. The regression equation and regression coefficient of EC<sub>10</sub>=62000 mg/l was calculated to  $y=0.0003x+6.9909$ ,  $R_2=0.9988$ , after 120 min photocatalytic oxidation time, at pH=7.0 and 60°C. The regression equation and regression coefficient of EC<sub>5</sub>=58000 mg/l was computed to  $y=0.000006x+1.6396$ ,  $R_2=0.9952$ , after 150 min photocatalytic oxidation time, at pH=7.0 and 60°C.

The EC<sub>90</sub> values decreased to EC<sub>50</sub>=60955 mg/l to EC<sub>25</sub>=43126 and to EC<sub>20</sub>=31168 mg/l after 60 min, 120 min and 150 min photocatalytic oxidation times, respectively, in Ni/Al<sub>2</sub>O<sub>3</sub>/TiO<sub>2</sub> NCs=50 mg/l at 30°C Table 8, SET 3. The

EC<sub>90</sub> values decreased to EC<sub>45</sub>=63188 mg/l to EC<sub>20</sub>=37713 and to EC<sub>15</sub>=23515 mg/l after 60 min, 120 min and 150 min photocatalytic oxidation times, respectively, in Ni/Al<sub>2</sub>O<sub>3</sub>/TiO<sub>2</sub> NCs=250 mg/l at 30°C. The EC<sub>90</sub> values decreased to EC<sub>55</sub>=54774 mg/l to EC<sub>30</sub>=34630 and to EC<sub>20</sub>=15280 mg/l after 60 min, 120 min and 150 min photocatalytic oxidation times, respectively, in Ni/Al<sub>2</sub>O<sub>3</sub>/TiO<sub>2</sub> NCs=1000 mg/l at 30°C.

The Microtox acute toxicity removals were 77.78%, 83.33% and 77.78% in 50, 250 and 1000 mg/l Ni/Al<sub>2</sub>O<sub>3</sub>/TiO<sub>2</sub> NCs, respectively, after 150 min photocatalytic oxidation time at 30°C. It was obtained an inhibition effect of Ni/Al<sub>2</sub>O<sub>3</sub>/TiO<sub>2</sub> NCs=1000 mg/l to *Aliivibrio fischeri* after 150 min photocatalytic oxidation time at 30°C Table 8, SET 3.

No	Parameters	Microtox Acute Toxicity Values, * EC (mg/l)							
		25°C							
		0. min		60. min		120. min		150. min	
		*EC <sub>90</sub>		*EC		*EC		*EC	
1	Raw OMW, control	100000		EC <sub>80</sub> =90000		EC <sub>75</sub> =98000		EC <sub>70</sub> =95000	
		30°C				60°C			
		0	60	120	150	0	60	120. min	150. min
		min	min	min	min	min	min		
		*EC <sub>90</sub>	*EC	*EC	*EC	*EC <sub>90</sub>	*EC	*EC	*EC
2	Raw OMW, control	100000	EC <sub>75</sub> =90000	EC <sub>70</sub> =94000	EC <sub>60</sub> =95000	100000	EC <sub>70</sub> =65000	EC <sub>70</sub> =65000	EC <sub>50</sub> =60000
3	Ni/Al <sub>2</sub> O <sub>3</sub> /TiO <sub>2</sub> NCs = 50 mg/l	100000	EC <sub>50</sub> =60955	EC <sub>25</sub> =43126	EC <sub>20</sub> =31168	100000	EC <sub>45</sub> =67776	EC <sub>20</sub> =43439	EC <sub>15</sub> =29255
	Ni/Al <sub>2</sub> O <sub>3</sub> /TiO <sub>2</sub> NCs = 250 mg/l	100000	EC <sub>45</sub> =63188	EC <sub>20</sub> =37713	EC <sub>15</sub> =23515	100000	EC <sub>40</sub> =55019	EC <sub>15</sub> =32326	EC <sub>10</sub> =49620
	Ni/Al <sub>2</sub> O <sub>3</sub> /TiO <sub>2</sub> NCs = 500 mg/l	100000	EC <sub>40</sub> =60316	EC <sub>15</sub> =37802	EC <sub>10</sub> =23804	100000	EC <sub>35</sub> =75000	EC <sub>10</sub> =62000	EC <sub>5</sub> =58000
	Ni/Al <sub>2</sub> O <sub>3</sub> /TiO <sub>2</sub> NCs = 1000 mg/l	100000	EC <sub>55</sub> =54774	EC <sub>30</sub> =34630	EC <sub>20</sub> =15280	100000	EC <sub>50</sub> =45350	EC <sub>25</sub> =30267	EC <sub>15</sub> =14580
* EC values were calculated based on COD <sub>dis</sub> (mg/l).									

**Table 8:** Effect of increasing Ni/Al<sub>2</sub>O<sub>3</sub>/TiO<sub>2</sub> NCs concentrations on Microtox acute toxicity in OMW at 30°C and at 60°C.

The EC<sub>90</sub> values decreased to EC<sub>45</sub>=67776 mg/l to EC<sub>20</sub>=43439 and to EC<sub>15</sub>=29255 mg/l after 60 min, 120 min and 150 min photocatalytic oxidation times, respectively, in Ni/Al<sub>2</sub>O<sub>3</sub>/TiO<sub>2</sub> NCs=50 mg/l at 60°C Table 8, SET 3. The EC<sub>90</sub> values decreased to EC<sub>40</sub>=55019 mg/l to EC<sub>15</sub>=32326 and to EC<sub>10</sub>=49620 mg/l after 60 min, 120 min and 150 min photocatalytic oxidation times, respectively, in Ni/Al<sub>2</sub>O<sub>3</sub>/TiO<sub>2</sub> NCs=250 mg/l at 60°C. The EC<sub>90</sub> values decreased to EC<sub>50</sub>=45320 mg/l to EC<sub>25</sub>=30267 and to EC<sub>15</sub>=14580 mg/l after 60 min, 120 min and 150 min photocatalytic oxidation times, respectively, in Ni/Al<sub>2</sub>O<sub>3</sub>/TiO<sub>2</sub> NCs=1000 mg/l at 60°C. The Microtox acute toxicity removals were 83.33%, 88.89% and 83.33% in 50, 250 and 1000 mg/l Ni/Al<sub>2</sub>O<sub>3</sub>/TiO<sub>2</sub> NCs, respectively, after 150 min photocatalytic oxidation time at 60°C. It was observed an inhibition effect of Ni/Al<sub>2</sub>O<sub>3</sub>/TiO<sub>2</sub> NCs=1000 mg/l to *Aliivibrio fischeri* after 150 min photocatalytic oxidation time at 60°C Table 8, SET 3.

Increasing Ni/Al<sub>2</sub>O<sub>3</sub>/TiO<sub>2</sub> NCs concentrations (from 50 to 1000 mg/l) were applied to the Microtox acute toxicity test Table 8, SET 3). The maximum acute toxicity removal was found at 500 mg/l Ni/Al<sub>2</sub>O<sub>3</sub>/TiO<sub>2</sub> NCs concentrations after 150 min photocatalytic oxidation time at 60°C. High Ni/Al<sub>2</sub>O<sub>3</sub>/TiO<sub>2</sub> NCs (> 500 mg/l) concentrations caused to the inhibition effect of *Aliivibrio fischeri* during Microtox acute toxicity assay. Low acute toxicity yield was measured above 500 mg/l Ni/Al<sub>2</sub>O<sub>3</sub>/TiO<sub>2</sub> NCs concentrations and low photocatalytic oxidation temperature (30°C) Table 8, SET 3.

### Effect of Ni/Al<sub>2</sub>O<sub>3</sub>/TiO<sub>2</sub> NCs Concentrations on the *Daphnia magna* Acute Toxicity Removal Efficiencies in OMW at Increasing Photo-oxidation Time and Temperature

The initial EC<sub>50</sub> values were observed as 78000 mg/l at 25°C Table 9, SET 1. The regression equation and regression



coefficient of raw OMW, (control or blank sample) for  $EC_{50}$ =78000 mg/l was computed to  $y=0.0006x+1.3269$ ,  $R_2=0.9954$ , at pH=7.0 and 25°C. After 60 min, 120 min and 150 min of photocatalytic oxidation times the  $EC_{50}$  values decreased to  $EC_{30}$ =50000 mg/l to  $EC_{20}$ =40000 mg/l and

to  $EC_{10}$ =24000 mg/l in Ni/Al<sub>2</sub>O<sub>3</sub>/TiO<sub>2</sub> NCs =500 mg/l at 30°C Table 9, SET 3. The toxicity removal efficiencies were 40%, 60% and 80% after 60 min, 120 min and 150 min photocatalytic oxidation times, respectively, in Ni/Al<sub>2</sub>O<sub>3</sub>/TiO<sub>2</sub> NCs=1000 mg/l at 30°C Table 9, SET 3.

No	Parameters	Daphnia magna acute toxicity values, *EC (mg/l)							
		25°C							
		0. min		60. min		120. min		150. min	
		*EC <sub>50</sub>		*EC		*EC		*EC	
1	Raw OMW, control	78000		EC <sub>40</sub> =85000		EC <sub>30</sub> =55000		EC <sub>25</sub> =39000	
		30°C				60°C			
		0. min	60 min	120. min	150. min	0. min	60 min	120. min	150. min
		*EC <sub>50</sub>	*EC	*EC	*EC	*EC <sub>50</sub>	*EC	*EC	*EC
2	Raw OMW, control	78000	EC <sub>35</sub> =70000	EC <sub>30</sub> =65000	EC <sub>25</sub> =40000	78000	EC <sub>30</sub> =60000	EC <sub>25</sub> =37000	EC <sub>20</sub> =29000
3	Ni/Al <sub>2</sub> O <sub>3</sub> /TiO <sub>2</sub> NCs =50 mg/l	78000	EC <sub>35</sub> =60000	EC <sub>25</sub> =32500	EC <sub>15</sub> =37500	78000	EC <sub>30</sub> =29000	EC <sub>20</sub> =60000	EC <sub>10</sub> =44000
	Ni/Al <sub>2</sub> O <sub>3</sub> /TiO <sub>2</sub> NCs =250 mg/l	78000	EC <sub>35</sub> =60000	EC <sub>25</sub> =27500	EC <sub>15</sub> =20000	78000	EC <sub>30</sub> =57500	EC <sub>20</sub> =27500	EC <sub>5</sub> =20000
	Ni/Al <sub>2</sub> O <sub>3</sub> /TiO <sub>2</sub> NCs =500 mg/l	78000	EC <sub>30</sub> =50000	EC <sub>20</sub> =40000	EC <sub>10</sub> =24000	78000	EC <sub>30</sub> =37000	EC <sub>15</sub> =21500	EC <sub>5</sub> =9750
	Ni/Al <sub>2</sub> O <sub>3</sub> /TiO <sub>2</sub> NCs =1000 mg/l	78000	EC <sub>35</sub> =45000	EC <sub>25</sub> =32500	EC <sub>20</sub> =22000	78000	EC <sub>30</sub> =34000	EC <sub>20</sub> =24000	EC <sub>15</sub> =6000
* EC values were calculated based on COD <sub>dis</sub> (mg/l)									

**Table 9:** Effect of increasing Ni/Al<sub>2</sub>O<sub>3</sub>/TiO<sub>2</sub> NCs concentrations on Daphnia magna acute toxicity in OMW at 30°C and at 60°C.

The  $EC_{50}$  values decreased to  $EC_{30}$  to  $EC_{15}$  and to  $EC_5$  after 60 min, 120 min and 150 min photocatalytic oxidation times, respectively, in Ni/Al<sub>2</sub>O<sub>3</sub>/TiO<sub>2</sub> NCs=500 mg/l at 60°C Table 9, SET 3. The  $EC_{30}$ , the  $EC_{15}$  and the  $EC_5$  values were measured as 37000 mg/l, 21500 and 9750 mg/l, respectively, in Ni/Al<sub>2</sub>O<sub>3</sub>/TiO<sub>2</sub> NCs=500 mg/l at 60°C. The toxicity removal efficiencies were 40%, 70% and 90% after 60 min, 120 min and 150 min photocatalytic oxidation times, respectively, in Ni/Al<sub>2</sub>O<sub>3</sub>/TiO<sub>2</sub> NCs=500 mg/l at 60°C Table 9, SET 3. 90% maximum Daphnia magna acute toxicity removal was obtained in Ni/Al<sub>2</sub>O<sub>3</sub>/TiO<sub>2</sub> NCs=500 mg/l after 150 min photocatalytic oxidation time at 60°C Table 9, SET 3).

The regression equation and regression coefficient of  $EC_{30}$ =37000 mg/l was calculated to  $y=0.001x-1.1097$ ,  $R_2=0.9974$ , after 60 min photocatalytic oxidation time, at pH=7.0 and 60°C. The regression equation and regression coefficient of  $EC_{15}$ =21500 mg/l was computed to  $y=0.0007x-0.1828$ ,  $R_2=0.9970$ , after 120 min photocatalytic oxidation time, at pH=7.0 and 60°C. The regression equation

and regression coefficient of  $EC_5$ =9750 mg/l was measured to  $y=0.0003x-0.0624$ ,  $R_2=0.9955$ , after 150 min photocatalytic oxidation time, at pH=7.0 and 60°C.

The  $EC_{50}$  values decreased to  $EC_{35}$ =60000 mg/l to  $EC_{25}$ =32500 and to  $EC_{15}$ =37500 mg/l after 60 min, 120 min and 150 min photocatalytic oxidation times, respectively, in Ni/Al<sub>2</sub>O<sub>3</sub>/TiO<sub>2</sub> NCs=50 mg/l at 30°C Table 9, SET 3. The  $EC_{50}$  values decreased to  $EC_{35}$ =60000 mg/l to  $EC_{25}$ =27500 and to  $EC_{15}$ =20000 mg/l after 60 min, 120 min and 150 min photocatalytic oxidation times, respectively, in Ni/Al<sub>2</sub>O<sub>3</sub>/TiO<sub>2</sub> NCs=250 mg/l at 30°C. The  $EC_{50}$  values decreased to  $EC_{35}$ =45000 mg/l to  $EC_{25}$ =32500 and to  $EC_{20}$ =22000 mg/l after 60 min, 120 min and 150 min photocatalytic oxidation times, respectively, in Ni/Al<sub>2</sub>O<sub>3</sub>/TiO<sub>2</sub> NCs=1000 mg/l at 30°C. The Daphnia magna acute toxicity removals were 70%, 70% and 60% in 50, 250 and 1000 mg/l Ni/Al<sub>2</sub>O<sub>3</sub>/TiO<sub>2</sub> NCs, respectively, after 150 min photocatalytic oxidation time at 30°C. It was observed an inhibition effect of Ni/Al<sub>2</sub>O<sub>3</sub>/TiO<sub>2</sub> NCs=1000 mg/l to Daphnia magna after



150 min photocatalytic oxidation time at 30°C Table 9, SET 3.

The  $EC_{50}$  values decreased to  $EC_{30}=29000$  mg/l to  $EC_{20}=60000$  and to  $EC_{10}=44000$  mg/l after 60 min, 120 min and 150 min photocatalytic oxidation times, respectively, in Ni/Al<sub>2</sub>O<sub>3</sub>/TiO<sub>2</sub> NCs=50 mg/l at 60°C Table 9, SET 3. The  $EC_{50}$  values decreased to  $EC_{30}=57500$  mg/l to  $EC_{20}=27500$  and to  $EC_5=20000$  mg/l after 60 min, 120 min and 150 min photocatalytic oxidation times, respectively, in Ni/Al<sub>2</sub>O<sub>3</sub>/TiO<sub>2</sub> NCs=250 mg/l at 60°C. The  $EC_{50}$  values decreased to  $EC_{30}=34000$  mg/l to  $EC_{20}=24000$  and to  $EC_{15}=6000$  mg/l after 60 min, 120 min and 150 min photocatalytic oxidation times, respectively, in Ni/Al<sub>2</sub>O<sub>3</sub>/TiO<sub>2</sub> NCs=1000 mg/l at 60°C. The *Daphnia magna* acute toxicity removals were 80%, 90% and 70% in 50, 250 and 1000 mg/l Ni/Al<sub>2</sub>O<sub>3</sub>/TiO<sub>2</sub> NCs, respectively, after 150 min photocatalytic oxidation time at 60°C. It was obtained an inhibition effect of Ni/Al<sub>2</sub>O<sub>3</sub>/TiO<sub>2</sub> NCs=1000 mg/l to *Daphnia magna* after 150 min photocatalytic oxidation time at 60°C Table 9, SET 3.

The maximum acute toxicity removals were approximately 90% at the Ni/Al<sub>2</sub>O<sub>3</sub>/TiO<sub>2</sub> NCs concentration of 500 mg/l at 60°C after 150 min of photocatalytic oxidation time Table 9, SET 3. Ni/Al<sub>2</sub>O<sub>3</sub>/TiO<sub>2</sub> NCs concentrations > 500

mg/l decreased the acute toxicity removals by hindering the photocatalytic oxidation process. Similarly, a significant contribution of increasing Ni/Al<sub>2</sub>O<sub>3</sub>/TiO<sub>2</sub> NCs concentration to acute toxicity removal at 60°C after 150 min of photocatalytic oxidation time was not observed. Low toxicity removals found at high Ni/Al<sub>2</sub>O<sub>3</sub>/TiO<sub>2</sub> NCs concentrations could be attributed to their detrimental effect on the *Daphnia magna* Table 9, SET 3.

### Direct Effects of Ni/Al<sub>2</sub>O<sub>3</sub>/TiO<sub>2</sub> NCs Concentrations on the Acute Toxicity of Microtox and *Daphnia Magna* in OMW

The acute toxicity test was performed in the samples containing 50 mg/l, 250 mg/l, 500 and 1000 mg/l Ni/Al<sub>2</sub>O<sub>3</sub>/TiO<sub>2</sub> NCs concentrations. In order to detect the direct responses of Microtox (with *Aliivibrio fischeri*) and *Daphnia magna* to the increasing Ni/Al<sub>2</sub>O<sub>3</sub>/TiO<sub>2</sub> NCs concentrations the toxicity test was performed without OMW. The initial EC values and the  $EC_{50}$  values were measured in the samples containing increasing Ni/Al<sub>2</sub>O<sub>3</sub>/TiO<sub>2</sub> NCs concentrations after 150 min photocatalytic oxidation time. Table 10 showed the responses of Microtox and *Daphnia magna* to increasing Ni/Al<sub>2</sub>O<sub>3</sub>/TiO<sub>2</sub> NCs concentrations.

Ni/Al <sub>2</sub> O <sub>3</sub> /TiO <sub>2</sub> NCs Conc. (mg/l)	Microtox Test			Daphnia Magna Test		
	Initial Acute Toxicity $EC_{50}$ Value (mg/l)	Inhibitions after 150 min	EC Values (mg/l)	Initial Acute Toxicity $EC_{50}$ Value (mg/l)	Inhibitions after 150 min	EC Values (mg/l)
50	$EC_{10}=25$	-	-	$EC_{10}=30$	-	-
250	$EC_{15}=150$	3	$EC_1=5.0$	$EC_{20}=200$	4	$EC_3=8.0$
500	$EC_{20}=200$	6	$EC_3=7.0$	$EC_{30}=250$	8	$EC_5=10.0$
1000	$EC_{25}=250$	8	$EC_7=11.0$	$EC_{40}=300$	10	$EC_9=20.0$

**Table 10:** The responses of Microtox and *Daphnia magna* acute toxicity tests in addition of increasing Ni/Al<sub>2</sub>O<sub>3</sub>/TiO<sub>2</sub> NCs concentrations without OMW after 150 min photocatalytic oxidation time.

The acute toxicity originating only from 50, 250, 500 and 1000 mg/l Ni/Al<sub>2</sub>O<sub>3</sub>/TiO<sub>2</sub> NCs were found to be low Table 10. 50 mg/l Ni/Al<sub>2</sub>O<sub>3</sub>/TiO<sub>2</sub> NCs did not exhibited toxicity to *Aliivibrio fischeri* and *Daphnia magna* before and after 150 min photocatalytic oxidation time. The toxicity attributed to the 50, 500 and 1000 mg/l Ni/Al<sub>2</sub>O<sub>3</sub>/TiO<sub>2</sub> NCs were found to be low in the samples without OMW for the test organisms mentioned above. The acute toxicity originated from the Ni/Al<sub>2</sub>O<sub>3</sub>/TiO<sub>2</sub> NCs decreased significantly to  $EC_1$ ,  $EC_3$  and  $EC_7$  after 150 min photocatalytic oxidation time. Therefore, it can be concluded that the toxicity originating from the Ni/Al<sub>2</sub>O<sub>3</sub>/TiO<sub>2</sub> NCs is not significant and the real acute toxicity throughout photocatalytic oxidation was attributed to the OMW, to their metabolites and to the photocatalytic oxidation by-products Table 10.

### Conclusion

The present study, the photooxidation of pollutant parameters (COD components, polyphenols and TAAs metabolites) in the OMW examined under UV-vis and sun light irradiations, with magnetic Ni/Al<sub>2</sub>O<sub>3</sub>/TiO<sub>2</sub> NCs, at optimum operational conditions. To the maximum yields of pollutant parameters {COD components [ $COD_{total}$ ,  $COD_{dis}$ ,  $COD_{inert}$ ], polyphenols [catechol, 3-hydroxybenzoic acid, tyrosol, 4-hydroxybenzoic acid, 4-hydroxyphenylacetic acid, 3-hydroxyphenylpropionic acid, 4-hydroxyphenylpropionic acid, 3,4-dihydroxyphenylethanol, 3,4-dihydroxyphenylacetic acid], polyaromatics [aniline, 4-nitroaniline, o-toluidine, o-anisidine, benzene, nitrobenzene, ethylbenzene, 3,6-bis(dimethylamino)durene, benzidine, dimethylaniline,

3,3-dichlorobenzidine], respectively} in the OMW reached, under 500 W UV-vis and 50 W sun lights, at 500 mg/l Ni/Al<sub>2</sub>O<sub>3</sub>/TiO<sub>2</sub> NCs, at a mass ratio of 1%/10%/5%, at pH=9.0, at 50°C, after 100 min, respectively. Under the optimized conditions, the maximum COD<sub>dis</sub>, total phenol and TAAs photooxidation yields were 98%, 88%, 94%, respectively, at pH=9.0, at 500 mg/l Ni/Al<sub>2</sub>O<sub>3</sub>/TiO<sub>2</sub> NCs, under 500 W UV-vis light, after 100 min photooxidation time, at 50°C, respectively. The maximum yields of total phenols and polyphenols; such as, catechol, 3-hydroxybenzoic acid, tyrosol, 4-hydroxybenzoic acid, 4-hydroxyphenylacetic acid, 3-hydroxyphenylpropionic acid, 4-hydroxyphenylpropionic acid, 3,4-dihydroxyphenylethanol, 3,4-dihydroxyphenylacetic acid in the OMW were 88%, 87%, 86%, 88%, 83%, 86%, 85%, 88%, 88% and 87%, respectively, under 500 W UV-vis light, at 500 mg/l Ni/Al<sub>2</sub>O<sub>3</sub>/TiO<sub>2</sub> NCs, at 1%/10%/5% mass ratio of Ni/Al<sub>2</sub>O<sub>3</sub>/TiO<sub>2</sub>, at pH=9.0, at 50°C, after 100 min, respectively. The maximum removal efficiencies of TAAs and TAAs metabolites; such as, aniline, 4-nitroaniline, o-toluidine, o-anisidine, benzene, nitrobenzene, ethylbenzene, 3,6-bis(dimethylamino)durene, benzidine, dimethylaniline, 3,3-dichlorobenzidine in the OMW were 94%, 92%, 90%, 91%, 89%, 88%, 93%, 92%, 85%, 93%, 89% and 90%, respectively, under 500 W UV-vis light, at 500 mg/l Ni/Al<sub>2</sub>O<sub>3</sub>/TiO<sub>2</sub> NCs, at 1%/10%/5% mass ratio of Ni/Al<sub>2</sub>O<sub>3</sub>/TiO<sub>2</sub>, at pH=9.0, at 50°C, after 100 min, respectively Table 5. The photooxidation yields in the OMW under sun light was lower than the photooxidation yields in the OMW under UV-vis light.

94.44% maximum Microtox acute toxicity yield was found in Ni/Al<sub>2</sub>O<sub>3</sub>/TiO<sub>2</sub> NCs=500 mg/l after 150 min photocatalytic oxidation time at 60°C. 90% maximum Daphnia magna acute toxicity removal was obtained in Ni/Al<sub>2</sub>O<sub>3</sub>/TiO<sub>2</sub> NCs=500 mg/l after 150 min photocatalytic oxidation time at 60°C. Therefore, it can be concluded that the toxicity originating from the Ni/Al<sub>2</sub>O<sub>3</sub>/TiO<sub>2</sub> NCs is not significant and the real acute toxicity throughout photocatalytic oxidation was attributed to the OMW, to their metabolites and to the photocatalytic oxidation by-products. Microtox (with *Aliivibrio fischeri*) acute toxicity test was more sensitive than Daphnia magna acute toxicity assay.

Ni/Al<sub>2</sub>O<sub>3</sub>/TiO<sub>2</sub> NCs is suitable for photooxidation of polyphenols and TAAs metabolites in the OMW. The high removal efficiency obtained with Ni/Al<sub>2</sub>O<sub>3</sub>/TiO<sub>2</sub> NCs qualifies that this effect may be caused by the synergetic effect on the interface of Al<sub>2</sub>O<sub>3</sub>/TiO<sub>2</sub> and Ni that can promote the photo-induced electron mobility in the surface of TiO<sub>2</sub> and the absorption of Ni particles that bring the high concentration of the OMW around TiO<sub>2</sub> particles. Providing such a combination could be a step toward the development of sustainable, reliable and cost-effective technology for the treatment of agro-industrial wastewaters, which demonstrate high innate

resistance to bio-degradability.

## Acknowledgement

This research study was undertaken in the Environmental Microbiology Laboratories at Dokuz Eylül University Engineering Faculty Environmental Engineering Department, Izmir, Turkey. The authors would like to thank this body for providing financial support.

## References

1. Sole MM, Pons L, Conde M, Gaidau C, Baccardit A (2021) Characterization of Wet Olive Pomace Waste as Bio Based Resource for Leather Tanning. *Materials (Basel)* 14(19): 5790.
2. Atanassova D, Kefalas P, Petrakis C, Mantzavinos D, Kalogerakis N, et al. (2005) Sonochemical Reduction of the Antioxidant Activity of Olive Mill Wastewater. *Environ Int* 31(2): 281-287.
3. Paraskeva P, Diamadopoulou E (2006) Technologies for Olive Mill Wastewater (OMW) Treatment: a Review. *J Chem Technol Biotechnol* 81(9): 1475-1485.
4. Silva AMT, Nouli E, Carmo-Apolinario AC, Xekoukoulotakis P, Mantzavinos D (2007) Sonophotocatalytic/H<sub>2</sub>O<sub>2</sub> Degradation of Phenolic Compounds in Agro-Industrial Effluents. *Catalysis Today* 124(3-4): 232-239.
5. Lafi WK, Shannak B, Al-Shannag M, Al-Anber Z, Al-Hasan M (2009) Treatment of Olive Mill Wastewater by Combined Advanced Oxidation and Biodegradation. *Separation and Purification Technology* 70(2): 141-146.
6. Galloni MG, Ferrara E, Falletta E, Bianchi CL (2022) Olive Mill Wastewater Remediation: From Conventional Approaches to Photocatalytic Processes by Easily Recoverable Materials. *Catalysts* 12(8): 923.
7. Paredes C, Cegarra J, Roig A, Sanchez MMA, Bernal MP (1999) Characterisation of Olive Mill Wastewater (alpechin) and its Sludge for Agricultural Purposes. *Bioresource Technology* 67(2): 111-115.
8. Paraskeva P, Diamadopoulou E (2006) Technologies for Olive Mill Wastewater (OMW) Treatment: A Review. *Journal of Chemical Technology and Biotechnology* 81(9): 1475-1485.
9. Potoglou D, Kouzeli KA, Haralambopoulos D (2004) Solar Distillation of Olive Mill Wastewater. *Renewable Energy* 29(4): 569-579.
10. Caputo AC, Scacchia F, Pelagagge PM (2003) Disposal

- of By-Products in Olive Oil Industry: Waste-to-Energy Solutions. *Applied Thermal Engineering* 23(2): 197-214.
11. Niaounakis M, Halvadakis, Constantinos P (2004) Olive-Mill Waste Management: Literature Review and Patent Survey. Typothito-George Dardanos, Athens, Greece.
  12. Lucas MS, Peres JA (2009) Removal of COD from Olive Mill Wastewater by Fenton's Reagent: Kinetic Study. *J Hazard Mater* 168(2-3): 1253-1259.
  13. Stoller M, Bravi M (2010) Critical Flux Analyses on Differently Pretreated Olive Vegetation Wastewater Streams: Some Case Studies. *Desalination* 250(2): 578-582.
  14. Papaphilippou PC, Yiannapas C, Politi M, Daskalaki VM, Michael C, et al. (2013) Sequential Coagulation-Flocculation, Solvent Extraction and Photo-Fenton Oxidation for the Valorization and Treatment of Olive Mill Effluent. *Chemical Engineering Journal* 224: 82-88.
  15. Aziz KHH (2019) Application of Different Advanced Oxidation Processes for the Removal of Chloroacetic Acids using a Planar Falling Film Reactor. *Chemosphere* 228: 377-383.
  16. Aziz KHH, Omer KM, Mahyar A, Miessner H, Mueller S, et al. (2019) Application of Photocatalytic Falling Film Reactor to Elucidate the Degradation Pathways of Pharmaceutical Diclofenac and Ibuprofen in Aqueous Solutions. *Coatings* 9(8): 465.
  17. Djellabi R, Giannantonio R, Falletta E, Bianchi CL (2021) SWOT Analysis of Photocatalytic Materials towards Large Scale Environmental Remediation. *Current Opinion in Chemical Engineering* 33: 100696.
  18. Galloni MG, Cerrato G, Giordana A, Falletta E, Bianchi CL (2022) Sustainable Solar Light Photodegradation of Diclofenac by Nano- and Micro-Sized SrTiO<sub>3</sub> Catalysts 12(8): 804.
  19. Azzam MOJ, Al-Malah KI, Abu-Lail NI (2004) Dynamic Post-Treatment Response of Olive Mill Effluent Wastewater using Activated Carbon. *Journal of Environmental Science and Health, Part A Toxic/Hazardous Substances and Environmental Engineering* 39(1): 269-280.
  20. Justino CI, Duarte K, Loureiro F, Pereira R, Antunes SC, et al. (2009) Toxicity and Organic Content Characterization of Olive Oil Mill Wastewater Undergoing a Sequential Treatment with Fungi and Photo-Fenton Oxidation. *J Hazard Mater* 172: 1560-1572.
  21. Sabbah I, Marsook T, Basheer S (2004) The Effect of Pretreatment on Anaerobic Activity of Olive Mill Wastewater using Batch and Continuous Systems. *Process Biochemistry* 39(12): 1947-1951.
  22. Hajjouji EIH, Merlina G, Pinelli E, Winterton P, Revel JC, et al. (2008) <sup>13</sup>C NMR Study of the Effect of Aerobic Treatment of Olive Mill Wastewater (OMW) on its Lipid-Free Content. *J Hazard Mater* 154(1-3): 927-932.
  23. Francioso O, Ferrari E, Saladini M, Montecchio D, Giocchini P, et al. (2007) TG-DTA, DRIFT and NMR Characterisation of Humic-Like Fractions from Olive Wastes and Amended Soil. *Journal of Hazardous Materials* 149(2): 408-417.
  24. Hafidi M, Amira S, Revel JC (2005) Structural Characterization of Olive Mill Waster-Water after Aerobic Digestion using Elemental Analysis, FTIR and <sup>13</sup>C NMR. *Process Biochemistry* 40(8): 2615-2622.
  25. Kallel M, Belaid C, Boussahel R, Ksibi M, Montiel A, et al. (2009) Olive Mill Wastewater Degradation by Fenton Oxidation with Zero-Valent Iron and Hydrogen Peroxide. *J Hazard Mater* 163(2-3): 550-554.
  26. Kallel M, Belaid C, Mechichi T, Ksibi M, Elleuch B (2009) Removal of Organic Load and Phenolic Compounds from Olive Mill Wastewater by Fenton Oxidation with Zero-Valent Iron. *Chemical Engineering Journal* 150(2): 391-395.
  27. Uğurlu M, Karaoglu MH (2011) TiO<sub>2</sub> Supported on Sepiolite: Preparation, Structural and Thermal Characterization and Catalytic Behaviour in Photocatalytic Treatment of Phenol and Lignin from Olive Mill Wastewater. *Chemical Engineering Journal* 166(3): 859-867.
  28. Gioia DD, Fava F, Bertin L, Marchetti L (2001) Biodegradation of Synthetic and Natural Occurring Mixtures of Mono-Cyclic Aromatic Compounds Present in Olive Mill Wastewaters by Two Aerobic Bacteria. *Appl Microbiol Biotechnol* 55(5): 619-626.
  29. Khoufi S, Aloui F, Sayadi S (2009) Pilot Scale Hybrid Process for Olive Mill Wastewater Treatment and Reuse. *Chemical Engineering and Processing: Process Intensification* 48(2): 643-650.
  30. Pang H, Li Y, Guan L, Lu Q, Gao F (2011) TiO<sub>2</sub>/Ni Nanocomposites: Biocompatible and Recyclable Magnetic Photocatalysts. *Catalysis Communications* 12(7): 611-615.
  31. Lipps WC, Braun-Howland EB, Baxter TE (2022) Standard Methods for the Examination of Water and Wastewater,

- 24<sup>th</sup> (Edn.). American Water Works Association (AWWA) 800 I Street, NW Washington DC: 20001-3770, USA.
32. Germirli F, Orhon D, Artan N (1991) Assessment of the Initial Inert Soluble COD in Industrial Wastewaters. *Water Science & Technology* 23(4-6): 1077-1086.
  33. Lange B (1994) LUMISmini, Operating Manual. Dusseldorf, Germany.
  34. Lange B (2010) *Vibrio fischeri* -Microtox LCK 491 kit. Germany.
  35. Lange B (1996) LUMIXmini type luminometer. Dusseldorf.
  36. Zar JH (1984) *Biostatistical analysis*, Prentice-Hall, Englewood Cliffs.
  37. (2005) Statgraphics Centurion XV, StatPoint Inc, Herndon, VA, USA,.
  38. Tuan WH, Liu SM, Ho CJ, Lin CS, Yang TJ, et al. (2005) Preparation of Al<sub>2</sub>O<sub>3</sub>-TiO<sub>2</sub>-Ni Nanocomposite by Pulse Electric Current and Pressureless Sintering. *Journal of the European Ceramic Society* 25(13): 3125-3133.
  39. Osman AI, Elgarahy AM, Eltaweil AS, El-Monaem EMA, El-Aqapa HG, et al. (2023) Biofuel Production, Hydrogen Production and Water Remediation by Photocatalysis, Biocatalysis and Electrocatalysis. *Environmental Chemistry Letters* 21(3): 1315-1379.
  40. Osman AI, Skillen NC, Robertson PKJ, David W, Rooney DW, et al. (2020) Exploring the Photocatalytic Hydrogen Production Potential of Titania Doped with Alumina Derived from Foil Waste. *International Journal of Hydrogen Energy* 45(59): 34494-34502.
  41. Yang G, Li J, Wang G, Yashima M, Min S (2005) Influences of TiO<sub>2</sub> Nanoparticles on the Microstructure and Mechanical Behavior of Ce-TZP/Al<sub>2</sub>O<sub>3</sub> Nanocomposites. *J Mater Sci* 40(23): 6087-6090.
  42. Herrmann JM, Duchamp C, Karkmaz M, Hoai BT, Lachheb H, et al. (2007) Environmental Green Chemistry as Defined by Photocatalysis. *Journal of Hazardous Materials* 146(3): 624-629.
  43. Gelover S, Mondragon P, Jimenez A (2004) Titanium Dioxide Sol-Gel Deposited Over Glass and its Application as a Photocatalyst for Water Decontamination. *Journal of Photochemistry and Photobiology A: Chemistry* 165(1-3): 241-246.
  44. Evans AG (1990) Perspective on the Development of High-Toughness Ceramics. *Journal of the American Ceramic Society* 73(2): 187-206.
  45. Vassilakis C, Pantidou A, Psillakis E, Kalogerakis N, Mantzavinos D (2004) Sonolysis of Natural Phenolic Compounds in Aqueous Solutions: Degradation Pathways and Biodegradability. *Water Res* 38(13): 3110-3118.
  46. Priego-Capote F, Ruiz-Jimenez J, Castro MDLD (2004) Fast Separation and Determination of Phenolic Compounds by Capillary Electrophoresis-Diode Array Detection Application to the Characterisation of Alperujo after Ultrasound-Assisted Extraction. *J Chromatogr A* 1045(1-2): 239-246.
  47. Priego-Capote F, Castro LD (2006) Ultrasound-Assisted Levitation: Lab-on-a-Drop. *TrAC Trends in Analytical Chemistry* 25(9): 856-867.
  48. Juarez MJB, Zafra-Gomez A, Luzon-Toro B, Ballesteros-Garcia OA, Navalon A, et al. (2008) Gas Chromatographyic-Mass Spectrometric Study of the Degradation of Phenolic Compounds in Wastewater Olive Oil by Azotobacter Chroococcum. *Bioresour Technol* 99(7): 2392-2398.
  49. Rehorek A, Tauber M, Gubitz G (2004) Application of Power Ultrasound for azo Dye Degradation. *Ultrason Sonochem* 11(3-4): 177-182.